UNIVERSITY OF CALIFORNIA, SAN DIEGO

Phosphorylation of Parkin by the autophagy initiating kinase ULK1 regulates mitochondrial homeostasis

A dissertation submitted in partial satisfaction of the requirements for the degree Doctor of Philosophy

in

Biology

by

Portia S. Lombardo

Committee in charge:

Professor Reuben J. Shaw, Chair
Professor Eric Bennett
Professor Åsa Gustafsson
Professor Randolph Hampton
Professor Amy Kiger

2017

The Dissertation of Portia S. Lombardo is approved, and is acceptable in quality and form for publication on microfilm and electronically:

_____

_____

_____

_____

_____

Chair

University of California, San Diego

2017

TABLE OF CONTENTS

LIST OF FIGURES

ACKNOWLEDGEMENTS

I would like to thank Reuben Shaw first and foremost for his mentorship and dedication throughout the course of my Ph.D. research. I am also grateful to Reuben for encouraging a lab environment that is both socially and scientifically engaging, as the Shaw Lab has fostered personal and professional relationships that I am thankful for.

I would like to thank my friends and family for all their support.

And I would especially like to thank Rob, for everything.

Chapter Two, in part, is currently being prepared for submission for publication of the material. Lombardo, Portia S.; Hellberg, Kristina; Garcia, Daniel; Brun, Sonja N.; Shaw, Reuben J. Portia S. Lombardo was the primary investigator and author of this paper.

VITA

EDUCATION:

University of California, San Diego, La Jolla, CA
Ph.D. in Biology. 2017.

Dartmouth College, Hanover, NH
A.B. in Biophysical Chemistry, *cum laude*. 2008.

ABSTRACT OF THE DISSERTATION

Phosphorylation of Parkin by the autophagy initiating kinase ULK1 regulates mitochondrial homeostasis

by

Portia S. Lombardo

Doctor of Philosophy in Biology

University of California, San Diego 2017

Professor Reuben Shaw, Chair

Our laboratory recently identified the autophagy initiating kinase ULK1 as a novel AMPK substrate, which directly connects the highly conserved AMPK-mediated energy sensing pathway to the regulation of autophagy.

Genetic deletion of ULK1 led to an accumulation of mitochondria with abnormal morphology, supporting a role for ULK1 kinase activity in the maintenance of mitochondrial homeostasis, yet few mammalian ULK1 substrates have been identified beyond those involved in the canonical initiation of autophagy. Here we have identified and validated the E3 ligase Parkin, a known mediator of mitochondrial quality control and the most commonly mutated gene in autosomal recessive early-onset Parkinson's disease, as a direct ULK1 substrate. ULK1-mediated phosphorylation of Parkin was required for maximal Parkin activity in multiple assays of Parkin function. These data reveal an important role for ULK1-mediated Parkin phosphorylation in the regulation of mitochondrial homeostasis, as this modification seems to prime Parkin for maximal activity following depolarization. Further studies using mouse models have indicated that Parkin is phosphorylated *in vivo* in mouse livers and primary hepatocytes in response to activators of the AMPK/ULK1 pathway, including Metformin, the most widely prescribed drug for the treatment of Type II diabetes. These data suggest the potential for profound *in vivo* relevance for the regulation of Parkin function downstream of the AMPK/ULK1 signaling cascade.

CHAPTER ONE:

Introduction to the AMPK/ULK1 signaling pathway and Parkin-mediated mitophagy

The AMPK signaling pathway is a master cellular energy regulator

The AMP-activated protein kinase (AMPK) is a highly conserved kinase complex which acts as a sensor and regulator of cellular energy homeostasis. As a kinase, the catalytic function of AMPK is to mediate the transfer of a phosphate group to a specific amino acid residue of a target protein substrate. This activity, known as phosphorylation, can subsequently alter the activity of the target substrate in a variety of different ways, including modulation of the substrates own enzymatic activity (either increasing or decreasing activity), changing its subcellular localization, or altering its local interacting partners. In this way, kinase activity sets off a series of changes in multiple downstream targets, referred to as a signaling pathway or cascade. Although 518 different kinases have been identified in the human genome (1), AMPK is uniquely positioned as a finely tuned sensor of cellular energy status due to its ability to directly bind the adenine nucleotides AMP, ADP, and ATP competitively. The AMPK complex is heterotrimeric, comprised of an α, β, and γ subunit, each of which is required for the important functions of the AMPK holoenzyme, which our laboratory has recently reviewed (2). The α subunit provides the catalytic activity, as it contains the kinase domain, as well as a conserved residue (Thr172) in the activation loop whose phosphorylation (by either of its upstream kinases, LKB1 or CAMKK2) is required for maximal AMPK activity. The β subunit contains a carbohydrate binding module and a myristoylation site, which are involved in glycogen sensing and intracellular

targeting, respectively, as well as domains for binding both the α and γ subunits. The γ subunit controls AMPK's energy-sensing ability, as it contains four cystathionine β-synthase repeats (comprising two Bateman domains), each of which may competitively bind the adenine nucleotides AMP, ADP, or ATP. The relative abundance of these molecules is modulated by energy status of the cell (with energy stress raising the ratio of AMP:ATP), and the binding of these nucleotides in turn modulates AMPK function, via conformational changes that alter kinase activity as well as the accessibility of the activated phospho-Thr172 residue to phosphatases. When cellular AMP levels rise relative to ATP levels, the net effect is that AMPK becomes highly activated. This effect can be achieved by energy stress on a whole organismal level as well as a cellular level, as ATP levels are affected by a wide range of stressors, including low nutrient availability, hypoxia, exercise, fasting, and any compounds that interfere with mitochondrial ATP production, such as the most widely prescribed Type II diabetes drug, Metformin, which falls under the biguanide class of compounds that inhibit the mitochondrial electron transport chain. AMPK can also be activated by AMP mimetic compounds (such as AICAR, which is metabolized to the AMP mimetic ZMP), or by direct allosteric activators. Once activated by any of these methods, AMPK uses its kinase activity to phosphorylate its downstream substrates, initiating a signaling cascade that inhibits anabolic processes and activates catabolic processes in an effort to restore cellular energy homeostasis. The anabolic processes

inhibited by AMPK activation involve multiple biosynthetic pathways, including gluconeogenesis, fatty acid synthesis, protein synthesis, and sterol synthesis, while the catabolic processes activated by AMPK include glycolysis, glucose uptake, fatty acid oxidation, and autophagy. By affecting these crucial metabolic processes, AMPK has been designated a “master cellular energy regulator”, and is studied extensively due to its involvement in a wide variety of physiological and disease states, including diabetes, obesity, cancer, aging, exercise endurance, and stem cell fate, to name a few.

A screen for novel AMPK substrates identifies the autophagy initiating kinase ULK1

AMPK regulates such a wide range of metabolic processes due to its ability to target an incredibly diverse array of downstream substrates for phosphorylation. Our laboratory and others have identified a number of substrates phosphorylated by activated AMPK, which include members of pathways involved in protein synthesis, fatty acid synthesis and oxidation, as well as transcriptional control of glucose and lipid metabolism. These substrates themselves perform a wide range of different enzymatic and non-enzymatic cellular functions, as they include protein kinases, lipid kinases, transcription factors, lipogenic enzymes, scaffolding proteins, and many more. Multiple approaches to the identification of novel AMPK substrates have been carried out, but in our laboratory we have largely focused on an AMPK

substrate screen involving the development of an “optimal AMPK motif” in conjunction with other screening methods. The optimal AMPK motif describes the preferred amino acid residues found at defined positions relative to a central phosphoacceptor residue on a candidate substrate of direct AMPK-mediated phosphorylation. This motif was first described and published by our laboratory in 2008 (3), and since then has been used to validate a number of additional AMPK substrate candidates. One such candidate that emerged from our phosphorylation motif screen was the autophagy initiating kinase ULK1, which our laboratory published in 2011 (4) and was independently verified by the Guan laboratory (5), albeit with differences in the specific phosphorylated residues reported (reviewed in (6)). The validation of ULK1 as a *bona fide* AMPK substrate was significant in that it represented the first direct connection of AMPK-mediated energy-sensing activity to the process of autophagy.

The AMPK/ULK1 signaling pathway regulates autophagy and mitochondrial homeostasis

Most broadly, ‘autophagy’ refers to a number of processes that converge upon the degradation of cellular components in the lysosome, and will be used hereafter to describe (as is conventional in the literature) the process more specifically known as ‘macroautophagy,’ wherein cellular components are engulfed by a double-membrane vesicle which subsequently fuses with the lysosome. Given that the AMPK-mediated signaling cascade is

known to play a major role in the restoration of cellular energy levels, it is perhaps unsurprising that it also directly regulates the autophagy initiating kinase ULK1. Autophagy is a process activated under conditions of low nutrient availability in order to promote cell survival by a variety of mechanisms, including the liberation of amino acids for production of proteins essential for starvation adaptation, generation of TCA-cycle intermediates (which contribute to the restoration of ATP levels), and even the facilitation of gluconeogenesis in the liver (7).

The serine/threonine kinase ULK1 is the predominant isoform of the two mammalian homologs (ULK1 and ULK2) of the yeast autophagy-related protein 1 (ATG1). ULK1 is considered the core of the autophagy initiation complex —the most upstream component of the autophagic pathway— which is comprised of ULK1, the autophagy-related proteins Atg13 and Atg101, and the focal adhesion kinase family interacting protein of 200 kDa (FIP200). As described previously, our laboratory identified ULK1 as a direct target of AMPK kinase activity (4). Intriguingly, this study also demonstrated that AMPK-dependent phosphorylation of ULK1 was not only necessary for survival under nutrient-deficient conditions but also for the proper autophagic clearance of mitochondria, as ULK1-deficient cells displayed higher mitochondrial content and an increased number of morphologically abnormal mitochondria. However, very little is currently known about how ULK1 actually mediates the steps required to initiate autophagy, as few mammalian ULK1

substrates have been reported to date and even fewer which would seem to be involved in the maintenance of mitochondrial homeostasis. Our laboratory and others have begun to approach the study of ULK1 function through the determination of novel substrates of ULK1 kinase activity.

A screen for novel ULK1 substrates identifies Parkin

The earliest-identified substrates of ULK1 kinase activity were components of its own core complex controlling autophagy initiation: the regulatory subunits Atg13 (8, 9) and FIP200 (10), as well as autophosphorylation of ULK1 itself (11). At the time that this thesis research project was established in our laboratory, a number of additional mammalian ULK1 substrates were reported, including AMBRA1 (12), syntenin-1 (13), TAB2 (14), raptor (15), and even AMPK itself (16), which may represent a potential feedback loop of regulation, although other investigators have reported an inability to detect ULK1-dependent phosphorylation of AMPK (15). However, the investigations of these reported substrates did not characterize specific ULK1 phosphorylation sites, which leaves open the possibility that some of these observed phosphorylation events may be ULK1-dependent but not directly mediated by ULK1. One of the first and most extensive characterizations of directly ULK1-mediated phosphorylation was reported in 2013 by the Guan laboratory, which identified the autophagy nucleation complex protein Beclin-1 as a novel substrate of ULK1 phosphorylation (17).

Since that time, other specific residues of ULK1-mediated direct phosphorylation have been reported by our laboratory and others, with substrates including VPS34 (18), FUNDC1 (19), Atg14 (20), Sec16a (21), and Sec23a (22). These laboratories have utilized differing approaches to the identification of these phosphorylation sites, and thus the validity of each of these specific residues as *bona fide* ULK1 substrates is not well established. However, these studies all clearly indicate a great interest in the identification and characterization of novel ULK1 substrates, and our laboratory is not alone in considering the list of reported substrates as incomplete. There also remains a large gap in our knowledge of the functional significance of these modifications, and the temporal and spatial contexts in which they are regulated. The approach our laboratory has taken to dissect the role of ULK1 in autophagy initiation has begun with a screen to identify novel ULK1 substrates, with a particular interest in those which may help explain the abnormal mitochondrial phenotype we have observed in the context of ULK1 loss, described in (4). In 2010, the Turk laboratory published a “large-scale” screening approach that identified putative phosphorylation motifs for half the kinases in the yeast kinome, including the optimal phosphorylation motif of Atg1, the yeast ortholog of mammalian ULK1 (23). However, this original Atg1 motif was generated using overexpressed Atg1 protein, which neglects to account for native Atg1 complex binding partners, and thus subsequent research further improved the motif by using the endogenous protein in its

native complex (24). Although Atg1 and ULK1 are closely related orthologs, our laboratory sought to generate an optimal phosphorylation motif specific to human ULK1, in order to identify putative substrates more likely to possess human physiological relevance. This motif analysis was initiated in a manner similar to our original AMPK substrate screen, as it involved the development of an optimal ULK1 phosphorylation consensus motif using the positional scanning peptide library technique described previously (3). The results of this phosphorylation motif analysis were reported by our laboratory in 2015 (18). Using this human ULK1 phosphorylation motif, we utilized Scansite (25) and PhosphoSitePlus (26), which are online systems biology based resources, in order to screen candidate substrates for the presence of ULK1 phosphorylation motifs. This approach not only identified specific residues of direct ULK1-mediated phosphorylation in previously reported substrates (including Atg101, Beclin1, AMBRA1, and Syntenin-1) and thereby increased our confidence in the validity of our screen, but also identified novel unreported substrates of human ULK1, including Vps34 (18) and Parkin. Since Parkin is a protein that has been shown to play a critical role in mitochondrial autophagy (referred to as mitophagy), the further validation and characterization of Parkin as a direct substrate of ULK1 was of great interest to our laboratory, and consequently formed the basis of the graduate thesis research described here.

Parkin mediates mitochondrial quality control via mitophagy

Since its discovery nearly twenty years ago, the Parkin gene has been a subject of wide-spread global interest. The gene, now known as PARK2, was first identified in 1998 as the causally mutated gene in Japanese patients with autosomal recessive juvenile parkinsonism (AR-JP) (27). Parkin mutations are now the leading known genetic cause of early-onset Parkinson's disease worldwide, representing 90% of all cases presenting before age 21 and 50% of cases presenting before age 45 (the age cutoff for early-onset designation) (28). Interest in Parkin has thus expanded rapidly, as it features in thousands of papers now published in the field and is the frequent subject of review (for recent reviews pertaining to the Parkin functions that will be described here, see (29-32)

Parkin is an E3 ubiquitin ligase (specifically of the RING between RING, or RBR, domain family), which means that the enzymatic function of activated Parkin is to ubiquitinate its downstream target substrates. As described previously, Parkin immediately captured our attention as an interesting potential novel substrate of ULK1, particularly in the context of the aberrant mitochondrial phenotype we observed following ULK1 loss, because it is already known to play an important role in the regulation of mitochondrial clearance, in a process conventionally referred to as PINK1/Parkin mediated mitophagy. In brief, this process of mitophagy is initiated by a decrease in mitochondrial membrane potential (indicative of damage to the mitochondrial

membrane), which blocks the import and cleavage of another kinase known as PINK1. This allows PINK1 to become stabilized on the outer mitochondrial membrane, where it can subsequently use its kinase activity to phosphorylate substrates at the mitochondrial surface. One such substrate of PINK1-mediated phosphorylation is ubiquitin itself, and this phosphorylated ubiquitin is thought to contribute to the recruitment of Parkin from the cytosol to the depolarized mitochondria. Following its recruitment to the mitochondria, Parkin can then also be phosphorylated by PINK1 at the Parkin Ser65 residue, which lies in Parkin's ubiquitin-like domain. Phosphorylation of Parkin by PINK1 at Ser65 is thought to contribute to activation of Parkin, by relieving Parkin from an autoinhibited conformation. Active Parkin then uses its E3 ligase activity to ubiquitinate outer mitochondrial membrane substrates, which are in turn phosphorylated by PINK1, leading to even more robust recruitment of Parkin and autophagic receptors, in what has been described as a "feed forward" mechanism (33). The recruitment of the autophagic machinery leads to the expansion of an autophagic membrane (termed the phagophore) which engulfs the damaged mitochondria into a double-membraned vesicle (autophagosome) that subsequently fuses with the lysosome to form an autolysosome, resulting in the degradation of the damaged mitochondria and constituting the final step of the process referred to as PINK1/Parkin mediated mitophagy.

Parkin as a novel substrate of ULK1

Parkin has emerged from our laboratory's screen to identify novel substrates of ULK1-mediated phosphorylation, and represents a very interesting new substrate of the AMPK/ULK1 signaling cascade for a number of reasons. On the most basic level, it expands our list of validated ULK1 substrates, of which few have been reported in mammalian systems, and thus contributes to our understanding of ULK1 function beyond its role in the canonical initiation of autophagy. More significantly, as a known mediator of mitochondrial quality control via its role in PINK1/Parkin mediated mitophagy, Parkin is an excellent candidate to explain the profound mitochondrial phenotype we observed in the absence of ULK1 kinase activity, and would thereby provide a piece of the molecular mechanism directly connecting energy sensing to mitophagy. The process of PINK1/Parkin mediated mitophagy is traditionally considered in the context of a cellular housekeeping role by promoting the turnover of isolated damaged mitochondria, but ULK1 activity downstream of AMPK activation would connect the highly conserved AMPK energy sensing response (which is activated by a wide range of stressors on both the organismal as well as cellular level) directly to the regulation of mitochondrial homeostasis. Furthermore, the identification of a novel phosphorylation site on Parkin represents a huge leap forward in our understanding of Parkin regulation. In spite of worldwide interest in the function and regulation of Parkin, to date the only extensively characterized

site of phosphorylation, or indeed of any posttranslational modification, on Parkin itself is the PINK1-mediated phosphorylation of Ser65. This phosphorylation event is directly downstream of mitochondrial depolarization, and thus ULK1-mediated phosphorylation of Parkin downstream of the AMPK/ULK1 energy sensing signaling cascade would represent an entirely new branch of regulation of Parkin. For these reasons, my graduate studies described in this thesis have aimed to validate Parkin as a novel substrate of ULK1.

CHAPTER TWO:

Phosphorylation of Parkin by the autophagy initiating kinase ULK1 regulates mitochondrial homeostasis

ABSTRACT

The AMP-activated protein kinase (AMPK) promotes cell survival during energy stress by phosphorylation of a diverse array of substrates that activate catabolic pathways or inhibit anabolic pathways. Our lab recently identified the autophagy initiating kinase ULK1 as a novel AMPK substrate, whose genetic deletion leads to an accumulation of mitochondria with abnormal morphology, supporting a role for ULK1 kinase activity in the maintenance of mitochondrial homeostasis. Here we identify the E3 ligase Parkin, a known mediator of autophagic clearance of damaged mitochondria (mitophagy) and the most commonly mutated gene in autosomal recessive early-onset Parkinson's disease, as a direct ULK1 substrate. ULK1 phosphorylates Parkin at multiple serine residues in response to activation of the AMPK/ULK1 signaling pathway, and we demonstrate that this phosphorylation is required for maximal Parkin activity following mitochondrial insult. Mutation of these phosphorylation sites in Parkin to non-phosphorylatable residues, as well as ULK1 loss or pharmacologic ULK1 inhibition, led to functional defects in multiple assays of Parkin activity, including decreased ubiquitination of Parkin substrates, delayed localization to damaged mitochondria, and defective mitochondrial clearance. We also observed phosphorylation of endogenous Parkin induced by the AMPK-pathway activating compound, and widely prescribed Type II diabetes drug, Metformin in mouse livers, as well as ULK1-dependent phosphorylation of endogenous Parkin in mouse primary

hepatocytes. These data reveal an important role for ULK1-mediated Parkin phosphorylation in the regulation of mitochondrial homeostasis *in vivo*.

INTRODUCTION

The unc-51 like autophagy initiating kinase (ULK1) is considered the major upstream initiator of the conserved intracellular degradative process known as autophagy, and is in fact the only known protein kinase involved in canonical autophagy initiation. Though the term autophagy encompasses multiple related processes, it is used here to describe the process of macro-autophagy, in which cellular components are engulfed in a double membrane vesicle known as the autophagosome, which subsequently fuses with the lysosome to degrade the cargo. Autophagy plays a crucial role in cellular housekeeping, as it facilitates the removal of damaged organelles, as well as in the cellular stress response, in order to promote cell survival during nutrient deprivation. In fact, ULK1 activity has been directly linked to the highly conserved AMP-activated protein kinase (AMPK) energy stress signaling cascade by AMPK-mediated phosphorylation of ULK1 at multiple residues (4, 5). In addition to identifying ULK1 phosphorylation sites induced by AMPK-activating stimuli, our laboratory also observed that phosphorylation of these residues was required for ULK1's ability to maintain mitochondrial homeostasis, as loss of this signaling either by ULK1 deficiency, inactivation of ULK1 kinase activity, or mutation of the AMPK-mediated phosphorylation sites

on ULK1 to non-phosphorylatable residues led to an aberrant accumulation of morphologically abnormal mitochondria (4). However, little is known to directly connect ULK1 to established regulators of mitochondrial quality control, as few direct substrates of ULK1 kinase activity have been identified in mammalian systems, and fewer beyond the canonical autophagic machinery. In addition to the cellular energy stress signals described previously, the AMPK/ULK1 signaling pathway is also robustly activated by mitochondrial insults, as any stressor that inhibits mitochondrial ATP production (including Metformin, the most widely prescribed Type II diabetes drug, which acts as an electron transport chain inhibitor) can activate this signaling cascade. Our laboratory has sought to identify novel components of the AMPK/ULK1 signaling pathway downstream of mitochondrial stress, with a particular interest in those which may contribute to the mitochondrial phenotype we have observed in the context of ULK1 loss. The approach our laboratory has taken to identify novel ULK1 substrates was initiated with the development of an optimal ULK1 kinase phosphorylation motif. The optimal phosphorylation motif of Atg1, the yeast ortholog of mammalian ULK1, was first described in 2010 as part of a large-scale screening approach that identified putative phosphorylation motifs for half the kinases in the yeast kinome, including overexpressed Atg1 (23). This Atg1 motif was further refined using the endogenous protein in its native complex and published in 2014 (24). Our laboratory sought to achieve a higher level of human physiological relevance by identifying substrates using an

optimal phosphorylation motif specifically designed toward human ULK1. This screen was performed using the positional scanning peptide library technique described previously (3), and the results of this phosphorylation motif analysis were reported by our laboratory in 2015 (18). Using this human ULK1 phosphorylation motif, we screened candidate substrates with a combination of bioinformatic and systems biology based resources available online, Scansite (25) and PhosphoSitePlus (26). This approach not only identified specific residues of direct ULK1 mediated phosphorylation in previously reported substrates (including Atg101, Beclin1, AMBRA1, and Syntenin-1) and thereby validated the robustness of our screen, but also identified novel unreported substrates of human ULK1, including Vps34 (18) and Parkin. The validation of Parkin as a potential novel substrate of ULK1 was of particular interest in the context of the aberrant mitochondrial phenotype we observed following ULK1 loss, as Parkin is an E3 ubiquitin ligase already known to play a crucial role in the selective clearance of damaged mitochondria (34). This process is now known as PINK1/Parkin mediated mitophagy (35, 36), and has been extensively reviewed, recently in (29-32). Parkin's role in this mitochondrial quality control process is especially significant in the context of human disease, as Parkin was first identified in 1998 as the causally mutated gene in Japanese patients with autosomal recessive juvenile parkinsonism (AR-JP) (27), and Parkin mutations are now the leading known genetic cause of early-onset Parkinson's disease worldwide, representing 50% of cases

presenting before age 45 (the age cutoff for early-onset designation) and 90% of all cases presenting before age 21 (28). Yet in spite of worldwide interest in the function and regulation of Parkin, to date the only extensively characterized site of phosphorylation on Parkin itself is the PINK1-mediated phosphorylation of the Ser65 residue (37, 38), which lies in Parkin's ubiquitin-like domain and is thought to contribute to activation of Parkin by relieving the protein from an autoinhibited conformation. Intriguingly, the only other extensively validated regulator of Parkin function is phosphorylated ubiquitin, which was discovered in 2014 by multiple independent investigators as a target of direct PINK1-mediated phosphorylation at the ubiquitin Ser65 residue (39-41). This phosphorylated ubiquitin directly binds to Parkin (42) and robustly contributes to Parkin activation. The discovery of ULK1-mediated Parkin phosphorylation sites is significant, as the process of PINK1/Parkin mediated mitophagy is traditionally considered in the context of a cellular housekeeping role by promoting the turnover of isolated damaged mitochondria, but ULK1-mediated Parkin phosphorylation downstream of AMPK activation would directly connect the highly conserved AMPK energy sensing response (which is activated by a wide range of stressors on both the organismal as well as cellular level) directly to the regulation of mitochondrial homeostasis. Here we report the identification of direct ULK1-mediated phosphorylation sites on Parkin, which are required for maximal Parkin activity

in multiple assays of Parkin function, revealing a novel regulation of mitochondrial quality control downstream of energy stress signaling.

RESULTS

Parkin S108-110 region identified as novel site of ULK1-dependent phosphorylation

In order to identify previously undiscovered substrates of ULK1 kinase activity, we generated an optimal ULK1 phosphorylation consensus motif, which uncovered multiple ULK1-dependent phosphorylation sites in several core autophagy pathway components, including Atg101, Beclin1, and VPS34, as described previously (18). In addition to these core members of the autophagy pathway, this screen also identified the E3 ligase Parkin as a novel candidate substrate of ULK1-mediated phosphorylation. In order to validate this putative substrate, we first utilized the overexpression of wildtype ULK1 in HEK293T cells, since the overexpressed kinase is constitutively active in this cell type. We observed a profound electrophoretic mobility shift of YFP-tagged human Parkin expressed in HEK293T cells on standard SDS-PAGE gels when co-expressed with Myc-tagged human ULK1 (WT ULK1), suggestive of phosphorylation (Figure 1A). This mobility shift was dependent on ULK1 kinase activity, as it was not observed following co-expression with Myc-ULK1 rendered kinase-inactive (KI ULK1) by a single point mutation, K46I. Furthermore, the Parkin bandshift induced by catalytically active WT ULK1

was diminished by treatment with lambda-phosphatase (Figure S1A). Mass spectrometry confirmed that Parkin is extensively phosphorylated upon co-expression with WT ULK1, and that these phosphorylation events are dramatically reduced following KI ULK1 co-expression (Figure 1B). Several of these phosphorylation sites likely represent secondary phosphorylation events that are induced by the presence of WT ULK1 but are not direct substrates of ULK1 itself *in vivo*. Of the sites identified by mass spectrometry, Parkin Ser108 and Ser110 also conform to the putative ULK1 motif displayed in previously identified ULK1 substrates (Figure 1C), indicating that these may be bona-fide direct substrates of ULK1 kinase activity. The Parkin Ser108-110 residues are notably well conserved in higher eukaryotes, with sequence homology observed back to *Caenorhabditis elegans* (Figure 1D). Intriguingly, phosphorylation of the homologous region in mouse Parkin was previously reported in an extensive phosphoproteomic dataset, with phosphorylation of this region identified as specifically induced in brown fat tissue (43). Thus phosphorylation of this region in mouse Parkin occurs within a metabolic tissue characterized by a high density of uncoupled mitochondria, lending support to the *in vivo* relevance of this region as a regulator of Parkin function. Importantly, although phosphorylation of this region was identified in mouse Parkin, the kinase responsible for mediating this phosphorylation was not identified, and we hypothesized that ULK1 could be a kinase directly regulating this region. Since our mass spectrometry results in human Parkin

(as well as those reported in mouse Parkin by Huttlin et al.) indicated that any of the Parkin 108-110 serines may be phosphorylated, and thus Ser-to-Ala mutation of one residue may be compensated for by phosphorylation of the adjacent residues, we generated constructs mutating all three serines in this region to alanines, which is subsequently abbreviated SA^3. Mutation of these serine residues to non-phosphorylatable alanines ablated the WT ULK1-induced bandshift, indicating that these are indeed significant sites of ULK1-mediated phosphorylation (Figure 1E). Additionally, mammalian expression constructs were generated containing Ser/Thr-to-Ala mutation of each phosphorylation site identified by mass spectrometry, regardless of their lack of conformation to the ULK1 motif, but only mutation of Ser108-110 completely ablated the WT ULK1 induced bandshift (Figure S1B).

Parkin S108-110 is phosphorylated *in vitro* and *in vivo*

In order to probe the regulation of Parkin S108-110 phosphorylation, we developed a phosphospecific antibody designed to detect phosphorylated Parkin Ser108, and thus subsequently referred to as 'pParkin S108.' The phospho-antibody detected robust signal by Western blotting in the presence of WT ULK1, which was not induced by KI ULK1, and mutation of the 108-110 serines to alanines caused the WT ULK1-induced signal to be entirely lost (Figure 2A). Although mutation of one of the Ser108-110 serines does not preclude the phosphorylation of the others, the antibody was unable to detect

signal in single-serine mutants (Figure S2A), indicating that the presence of all three serines is required for recognition by the phospho-antibody, but not sufficient for detection in the absence of phosphorylation induction. Given that phosphorylation of all three of the S108-110 residues was reported in our mass spectrometry results in the presence of WT ULK1, mutation of multiple residues was required to observe complete collapse of the WT ULK1-induced Parkin bandshift, and that this region is conserved and phosphorylated at multiple residues in mouse tissue (43), we will subsequently refer to phosphorylation detected by the pParkin S108 phosphoantibody as indicating phosphorylation of the Parkin S108-110 region. Neither Ser-to-Ala mutation of the Ser65 PINK1-induced Parkin phosphorylation site nor mutatgenesis of the commonly used representative Parkinson's disease mutation Lys161Asn affected the WT ULK1-induced phosphorylation of Parkin Ser108-110 (Figure S2B). To validate that ULK1 itself can directly mediate phosphorylation of Parkin, we performed *in vitro* kinase assays combining immunoprecipitated Myc-tagged Parkin with recombinant ULK1 protein and ATP. In these *in vitro* assays, the Parkin S108 phosphoantibody detected robust phosphorylation of Parkin, and these same assays also detected phosphorylation of the validated ULK1 substrate VPS34 using a phosphospecific antibody for the ULK1-mediated VPS34 phosphorylation site (Figure 2B, input controls Figure S2C). Having established that ULK1 can phosphorylate Parkin *in vitro*, we next sought to test the *in vivo* relevance of this phosphorylation by determining

whether phosphorylation of Parkin Ser108-110 occurs under conditions in which Parkin is known to be activated and whether this involves the induction of endogenous ULK1 kinase activity, in the absence of WT ULK1 overexpression. The mitochondrial depolarizing agent carbonyl cyanide m-chlorophenyl hydrazone (CCCP) has been frequently utilized to induce Parkin activity (32), and indeed we observed that CCCP rapidly induced phosphorylation of Parkin Ser108-110 in ULK1-expressing HEK293T cells, within 30 minutes of treatment (Figure 2C). Phosphorylation of ULK1 Ser555, considered an AMPK-mediated activating phosphorylation event (4, 44), is also increased by CCCP treatment. Depolarization-induced phosphorylation of Parkin Ser108-110 was also validated by mass spectrometry, which similarly detected this modification within 30 minutes of CCCP treatment (Figure S2D).

AMPK/ULK1 pathway activators induce phosphorylation of endogenous Parkin

Having identified novel sites of ULK1-mediated phosphorylation on Parkin using multiple overexpression systems, we sought to validate the presence of ULK1-dependent phosphorylation of endogenous Parkin using *in vivo* mouse model systems. As described previously, phosphorylation of the conserved mouse Parkin region was detected in a 2010 phosphoproteomic dataset, in which this phosphorylation of endogenous Parkin was observed in a tissue-specific manner in brown fat (43), though this dataset did not identify

the kinase mediating this phosphorylation. We have observed that brown fat tissue displays constitutively high levels of AMPK pathway activation (data not shown), which lends support to phosphorylation of this region downstream of active AMPK/ULK1 signaling, but does not facilitate the study of its regulation, as the pathway is already fully activated. Given our previous observation that ULK1 loss led to a defective mitochondrial phenotype in primary mouse hepatocytes (4), and our ability to examine AMPK/ULK1 pathway activation in mouse livers by injection of live mice with the AMPK-activating compound Metformin, we first focused on mouse livers for our investigation of endogenous Parkin regulation. Since the Parkin pS108 antibody was designed using a human Parkin target peptide, the phospho-antibody was unable to detect phosphorylation of these sites in mouse Parkin, and thus we relied on the Phos-tag acrylamide gel system to separate proteins based on phosphorylation status (45). When liver lysates were prepared from wildtype mice treated for 1 hour with Metformin, we observed the induction of ULK1 Ser555 phosphorylation, as well as a bandshift of endogenous Parkin on a Phos-tag acrylamide gel, indicating that Metformin activates the AMPK/ULK1 pathway and leads to phosphorylation of endogenous Parkin (Figure 2D). The Metformin-induced Parkin bandshift was completely ablated in AMPK-deleted mice, which have no ULK1 Ser555 phosphorylation in the absence of AMPK expression. To further probe the ULK1-dependence of this phosphorylation, we utilized ULK1/2 fl/fl mice with tail vein injection of AAV-Cre in an effort to

achieve liver-specific deletion of ULK1 and its closely related homologue ULK2. These mice were subsequently treated for 2 hours with Metformin, which again induced a bandshift of endogenous Parkin in the un-deleted (AAV-GFP) mouse livers, detected by Phos-tag acrylamide gel (Figure 2E). Under the conditions utilized, liver-specific ULK1 deletion by AAV-Cre was incomplete, and thus ULK1 levels were reduced yet Metformin treatment still stimulated a modest induction of ULK1 Ser555 phosphorylation. This reduced ULK1 activity corresponded to a reduced induction of Parkin phosphorylation, indicating that the Metformin-induced phosphorylation of endogenous Parkin is indeed downstream of ULK1 pathway activation.

Phosphorylation of S108-110 is required for maximal Parkin activity

Having identified novel Parkin phosphorylation sites induced in a WT ULK1 and stimulus-dependent manner, we next examined whether phosphorylation of these residues affects Parkin function. A number of functional assays have been widely used to characterize Parkin activity. One such readout is the ubiquitination of Parkin substrates, as activated Parkin uses its E3 ligase activity to ubiquitinate a wide range of proteins most frequently located at the outer mitochondrial membrane (46). MitoNEET and Mitofusin2 (Mfn2) are two well-validated substrates of Parkin ligase activity (47-49). MitoNEET ubiquitination is indicated here by higher-molecular weight forms of ubiquitinated MitoNEET detected by Western blotting, and these

forms increased in a time-dependent manner following a timecourse of CCCP treatment, indicating activated Parkin (Figure 3A). Mfn2 ubiquitination is indicated by the loss of Mfn2 protein, and this reduction is also induced by CCCP in a time-dependent manner. Both of these readouts of Parkin ligase activity are dramatically blunted when the Ser108-110 residues of Parkin are mutated to non-phosphorylatable alanines, similar to the defects observed upon mutation of the crucial Ser65 PINK1-induced phosphorylation site as well as a representative Parkinson's disease mutation previously demonstrated to display defective ligase activity (37). This indicates that phosphorylation of Parkin Ser108-110 is required for maximal CCCP-induced Parkin activity, as the loss of phosphorylation impairs the rate of ubiquitination of Parkin substrates.

CCCP treatment also induces translocation of Parkin from the cytosol to damaged mitochondria (34), and this recruitment has been widely used as an indicator of Parkin function. To investigate the effect of S108-110A mutation on this aspect of Parkin function, we generated mouse embryonic fibroblast (MEF) cell lines stably expressing either wildtype or mutant YFP-Parkin. Consistent with previously published results, we observed colocalization of wildtype Parkin with mitochondria within two hours of CCCP treatment (Figure 3B). CCCP treatment was also able to induce the mitochondrial colocalization of Ser108-110A mutant Parkin, as well as the PINK1 site mutant Ser65Ala and the representative Parkinson's disease mutant Lys161Asn, however, there

was less observed mitochondrial colocalization of mutant Parkin, with mutant Parkin remaining diffuse throughout the cytosol. These observations were quantified over a timecourse of CCCP treatment using previously described methods (35, 38), which confirmed that phosphorylation of the Ser108-110 ULK1 sites was required for optimal Parkin translocation to damaged mitochondria, as mutation of these sites to non-phosphorylatable alanines resulted in significantly fewer cells that displayed complete translocation of Parkin to damaged mitochondria, and significantly more cells that displayed no Parkin translocation whatsoever by 16 hrs of CCCP treatment (Figure 3C).

The previously described method of phenotypic scoring can also be employed to quantify the effects of Parkin mutation upon a third readout of Parkin function: the clearance of mitochondria in the final step of Parkin-mediated mitophagy, when the damaged mitochondria are degraded in the lysosome and thus not detected by immunofluorescence staining, leading to diffuse cytosolic Parkin in cells where the mitochondria appear absent (“gone”). Further confirming the importance of phosphorylation of Parkin Ser108-110, we observed that mutant Parkin expressing cells displayed significantly less mitochondrial clearance than cells expressing wildtype Parkin after 16 hours of CCCP treatment, and that mutant Parkin expressing cells also displayed a greater percentage of cells in which no Parkin colocalization or clearance of mitochondria was observed at all (Figure 3D). This delay in mitochondrial clearance in mutant Parkin expressing cells was also observable

by Western blot, in which a long timecourse of CCCP treatment induced loss of mitochondrially associated proteins (the outer mitochondrial membrane protein Tom20, as well as Complex IV and V components of the electron transport chain) in wildtype Parkin expressing cells, but this loss was blunted when the Ser108-110 residues were mutated to non-phosphorylatable alanines (Figure S3A).

Inhibition of ULK1 function decreases phosphorylation of Parkin and recapitulates the Parkin mutant phenotype

We predicted that if ULK1 is the major kinase responsible for phosphorylation of Parkin S108-110, then loss of ULK1 function should diminish phosphorylation of these residues, as well as phenocopy the reduced Parkin function we observed when S108-110 were mutated to non-phosphorylatable residues. To first establish the effect of ULK1 loss on phosphorylation of Parkin S108-110, we utilized siRNA pools targeting human ULK1, which greatly reduced ULK1 levels in HEK293T cells and importantly reduced the levels of CCCP-induced Parkin phosphorylation as well (Figure 4A). This reduction of ULK1 activity was also sufficient to reduce phosphorylation of Atg13, a well-characterized substrate of ULK1 (50, 51), indicated by the lower molecular weight mobility shift of unphosphorylated Atg13 in the siULK1 conditions. We also utilized a panel of additional AMPK/ULK1-pathway activating compounds, which each act in different ways

to induce or mimic energy stress, described subsequently, and observed that each of these compounds increased phosphorylation of ULK1 at Ser555 as well as induced phosphorylation of Parkin S108-110, and importantly that in all cases this phosphorylation was dramatically reduced by ULK1 knockdown. These compounds are expected to increase ULK1 phosphorylation and activity via activation of its upstream kinase, AMPK, by either a decrease in cellular ATP levels (Phenformin and Rotenone via electron transport chain inhibition, and Valinomycin via mitochondrial depolarization) or by direct allosteric activation (991;(52)). To further establish that phosphorylation of S108-110 has a functional effect on Parkin activity, we next sought to validate that this ULK1 knockdown-mediated loss of Parkin phosphorylation also correlated with decreased Parkin activity, consistent with the Parkin S108-110A mutant phenotype. We first examined the effect of siULK1 on ubiquitination of Parkin substrates, and observed that CCCP-induced ubiquitination of MitoNEET was decreased following ULK1 knockdown (Figure S4A). Furthermore, in immunofluorescence assays of Parkin activity, ULK1 siRNA knockdown also significantly delayed the translocation of Parkin to depolarized mitochondria over a short timecourse of CCCP treatment (Figure 4B), as well as significantly reduced the Parkin-mediated clearance of damaged mitochondria following prolonged treatment with CCCP (Figure 4C). These data indicate that loss of ULK1 activity by siRNA knockdown impairs phosphorylation of Parkin with a concomitant impairment of Parkin activity. To

further validate the effects of ULK1 loss of function on Parkin phosphorylation and activity, we utilized a newly developed small molecule inhibitor of ULK1 activity, SBI-0206965, hereafter referred to as “6965”, which was recently characterized by our laboratory (18). In this study, 6965 was identified as a highly selective ULK1 kinase inhibitor *in vitro* and inhibited the ability of endogenous ULK1 to phosphorylate ULK1 substrates. We tested the ability of 6965 to decrease CCCP- and 991-mediated phosphoryation of Parkin, and observed that co-treatment with 6965 dramatically reduced phosphorylation of S108-110 (Figure 4D), further supporting the role of ULK1 as the major kinase responsible for phosphorylation of this region. Inhibition of ULK1 by 6965 also recapitulated the effects observed following ULK1 siRNA knockdown or mutation of the Parkin S108-110 sites to non-phosphorylatable alanines, as co-treatment with 6965 impaired the ubiquitination of the Parkin substrate MitoNEET. 6965 treatment alone had no effect on phosphorylation of ULK1 Ser555, nor on Parkin phosphorylation or activity. The ability of 6965 to diminish CCCP-induced phosphorylation of Parkin S108-110 was additionally validated by mass spectrometry, which revealed phosphorylation of this region following CCCP treatment that was ablated by co-treatment of CCCP with 6965 (Figure S4B).

Similar to the Metformin-induced bandshift of endogenous Parkin in mouse livers observed previously, Phenformin (a Metformin analog with more potent activity in certain cell types), CCCP, as well as a combination of

antimycin and oligomycin (AO; a mitochondria-depolarizing combination) induced robust ULK1 Ser555 phosphorylation and a concomitant induction of phosphorylated endogenous Parkin in mouse primary hepatocytes (Figure S4C). Importantly, this phosphorylation of endogenous Parkin was reduced by co-treatment with the ULK1 inhibitor 6965, validating the ULK1-dependence of these phosphorylation events.

Genetic deletion of ULK1 reveals compensatory kinase activity to maintain phosphorylation of Parkin S108-110

Since loss of ULK1 function by both siRNA knockdown and a small molecule inhibitor decreased phosphorylation of the Parkin S108-110 region and blunted Parkin activity in a number of functional assays, we hypothesized that genetic deletion of ULK1 using the CRISPR/Cas9 system (Figure S5A) would produce similar results. However, unexpectedly, clonal cell populations established following targeting of ULK1 with the CRISPR/Cas9 system that appeared to have complete loss of ULK1 protein by Western blot frequently displayed CCCP-induced activation, or even hyperactivation, of Parkin activity and phosphorylation of Ser108-110 (Figure 5A). However, one of these clones (hereafter referred to as Clone B) revealed a much fainter band close in molecular weight to the endogenous ULK1 band of wildtype HEK293T cells, which exhibited signaling resembling ULK1 siRNA knockdown and 6965 ULK1 inhibitor treated cells, with diminished phosphorylation of S108-110 and a

corresponding reduction in Parkin activity demonstrated by the reduced ubiquitination of the Parkin substrate MitoNEET. Sequencing of Clone B revealed three different allelic mutations (the parental HEK293T cells are hypotriploid (53), two of which were out-of-frame (17 base pair insertion, and 22 base pair deletion) but one of which was in-frame (10 base pair insertion with one base pair deletion) (Figure 5B). The hypomorphic response observed in Clone B suggests that the single in-frame mutant ULK1 allele could provide sufficient ULK1 function for Clone B to avoid activation of compensatory kinases, yet is insufficient to achieve maximal ULK1 activity. The fact that phosphorylation of Parkin S108-110 was maintained in the ULK1-null clones suggested that phosphorylation of this region is indeed of great cellular importance, yet also raised the intriguing question of what kinase or kinases are activated to compensate for the loss of ULK1. We surmised that a natural candidate to fulfill this backup kinase role was the closely related kinase ULK2, which possesses an overall 52% amino acid identity to ULK1 as well as conserved domain structures, with the kinase domain being particularly well-conserved (76% amino acid identity) (54). There is also previous evidence for functional redundancy between ULK1 and ULK2, including the identification of multiple shared interacting partners, as well as the observations that both *ulk1*$^{-/-}$ mice and *ulk2*$^{-/-}$ mice are born viable yet *ulk1*$^{-/-}$ *ulk2*$^{-/-}$ mice display neonatal lethality, as reviewed in (55). Consistent with our hypothesis, qPCR for human ULK2 revealed a greater than two-fold induction of ULK2 expression in Clone

A compared to the wildtype parental cell line, while ULK2 expression in Clone B was unaffected (Figure 5C), suggesting that the Clone A ULK1-/- cells could compensate for loss of ULK1 by upregulation of the related ULK2 kinase. The role of ULK2 as a backup kinase in the context of ULK1 loss was further examined using the CRISPR/Cas9 method to knock out ULK2 in the wildtype and ULK1-/- HEK293T lines. In polyclonal populations of cells following targeting with CRISPR/Cas9 guides designed toward ULK2, targeting of ULK2 ablated the CCCP-induced phosphorylation of Parkin S108-110 in the hypercompensated Clone A line, with little apparent change in Parkin phosphorylation status in the wildtype or Clone B lines (Figure S5B). To confirm the ULK2-mediated specificity of this result, we directly compared this targeting of ULK2 to CRISPR/Cas9 guides designed toward TBK1, which we considered as another potential backup kinase due to its well-characterized involvement in mitophagy, where it is shown to be activated following mitochondrial depolarization and to directly mediate phosphorylation and regulation of the autophagic receptor Optineurin (56-58), as well its permissive phosphorylation motif (59). CRISPR/Cas9-mediated knockout of TBK1 was highly efficient in the polyclonal population, but loss of TBK1 did not affect phosphorylation of Parkin S108-110, indicating that the compensatory phosphorylation observed in ULK1-/- lines is not likely to be mediated by TBK1. Consistently, qPCR results did not detect any significant alterations in TBK1 expression levels in either Clone A or Clone B cells compared to

wildtype expression (Figure S5C). Taken together, the qPCR and CRISPR/Cas9 results strongly suggest that ULK2 acts as a backup kinase to maintain CCCP-induced phosphorylation of Parkin S108-110 in the ULK1-null context.

Energy stress primes Parkin for maximal activity following depolarization

Having identified that there is indeed an important biological significance to phosphorylation of Ser108-110 on Parkin activity in a number of functional assays, we next sought to determine whether this phosphorylation event was sufficient to drive Parkin activity *per se*. As described previously (see Figure 4A), a wide variety of compounds (including CCCP, Phenformin, Rotenone, 991, and Valinomycin) potently activate the AMPK/ULK1 pathway within one hour of treatment. This activation is observed in the induction of AMPK Thr172 phosphorylation and ULK1 Ser555 phosphorylation, and these compounds concomitantly induce phosphorylation of Parkin Ser108-110 (Figure 6A). INK128 is a selective inhibitor of mTOR, but this inhibition does not induce activation of AMPK or ULK1, and similarly does not induce phosphorylation of Parkin Ser108-110. Although all of the AMPK/ULK1 activating compounds described rapidly induce phosphorylation of Parkin Ser108-110, the ubiquitination of the Parkin substrate MitoNEET was only observed following treatment with the mitochondrial depolarizing agents

(CCCP and Valinomycin). When MEF cells stably expressing YFP-Parkin were examined by immunofluorescence, even prolonged (6 hr) treatment with the AMPK/ULK1 pathway activating compounds was insufficient to induce Parkin translocation to the mitochondria, unless this activation occurred in the presence of mitochondrial depolarization with CCCP or Valinomycin (Figure 6B). Taken together, these data indicate that activation of the AMPK/ULK1 pathway is required for Parkin Ser108-110 phosphorylation, but this phosphorylation is insufficient to drive Parkin activity towards mitophagy in the absence of depolarization. This contributes to our model wherein ULK1-mediated phosphorylation of Parkin Ser108-110 downstream of AMPK/ULK1 pathway activation primes Parkin for maximal activity in a number of functional assays (including mitochondrial translocation, substrate ubiquitination, and subsequent mitochondrial clearance) to promote robust mitophagy (Figure 6C).

DISCUSSION

As the most frequently mutated gene in autosomal recessive juvenile-onset Parkinson's disease, Parkin function has been widely studied, yet surprisingly little is known of its regulation *in vivo* beyond its well-characterized PINK1-mediated Ser65 phosphorylation site and interaction with phosphorylated ubiquitin. We have identified novel ULK1-mediated sites of Parkin phosphorylation in the S108-110 region, which are induced

downstream of the activated AMPK energy-sensing signaling cascade. Loss of S108-110 phosphorylation by mutation of this region to non-phosphorylatable residues, small-molecule inhibition of ULK1 activity, or ULK1 knockdown impairs Parkin activity in multiple assays of Parkin function, supporting the functional significance of these phosphorylation events. Thus phosphorylation of S108-110 downstream of AMPK/ULK1 pathway activation was required for efficient Parkin function following mitochondrial depolarization, suggesting that energy stress may act as a priming signal to promote maximal Parkin activity when combined with additional regulatory signals such as Ser65 phosphorylation. ULK1-mediated phosphorylation of Parkin S108-110 represents a novel direct connection between activation of the conserved energy-sensing AMPK pathway and mitochondrial quality control. Recent evidence has indicated that ULK1 can also phosphorylate the mitophagic receptor FUNDC1 at Ser318 (19), yet in spite of the longstanding observation that loss of ULK1 impairs mitochondrial morphology and clearance, there has been little other previous evidence to directly connect ULK1 to established regulators of mitophagy. Our laboratory also recently discovered that AMPK signaling controls another aspect of mitochondrial regulation through direct AMPK-mediated phosphorylation of the mitochondrial fission factor (MFF) (60), suggesting that AMPK can act through multiple arms of its signaling cascade to promote mitochondrial efficiency in response to energy stress. Although phosphorylation of S108-110 *per se* was insufficient to induce the

translocation of Parkin to mitochondria in the absence of depolarization, whether this phosphorylation affects alternative aspects of Parkin function, such as its activity toward cytosolic substrates (of which several have been reported (46)), has yet to be determined. Another significant finding that we report here is the *in vivo* phosphorylation of endogenous Parkin in response to AMPK/ULK1 pathway activation. In untreated mice, phosphorylation of the orthologous mouse region of Parkin was found to be specifically induced in brown fat (43), and although this study did not identify the kinase responsible for these phosphorylation events, it strongly indicated the importance of high metabolic activity (brown fat displays a high density of uncoupled mitochondria and robust AMPK pathway activation) on the regulation of Parkin in a tissue-specific manner. Our study presents exciting results in the context of treatment with AMPK pathway activating compounds, as we observed Metformin-induced phosphorylation of endogenous Parkin in mouse liver as well as ULK1-dependent phosphorylation of endogenous Parkin in primary mouse hepatocytes. The oral biguanide compound Metformin has been widely prescribed for the treatment of Type II diabetes since the mid-1970s, though astonishingly the compound itself is derived from the active ingredient of the French lilac *Galega officinalis*, also colloquially known as ‘Goat’s rue’, which was prescribed for the treatment of diabetic symptoms observed in medieval times (61). The beneficial effects of Metformin are known to be mediated in large part through activation of the AMPK signaling cascade (62, 63), and the

regulation of Parkin function downstream of active AMPK/ULK1 signaling presents a previously unappreciated role for mitochondrial quality control in the liver as well as in other metformin-responsive tissues. In fact, Metformin can cross the blood-brain barrier and is widely considered neuroprotective (64-66), though some controversy remains (67, 68), and thus merits thorough investigation. Intriguingly, *parkin* -/- mice are also susceptible to hepatocellular carcinoma (69), and Parkin has been proposed as a tumor suppressor in a number of human cancers (recently reviewed in (70)). In conclusion, our study has identified novel sites of human Parkin regulation directly downstream of AMPK/ULK1 pathway activation, and thus opens up several avenues for future investigation in important *in vivo* contexts, including Parkinson's disease, cancer, and diabetes.

EXPERIMENTAL PROCEDURES

Antibodies and Reagents

Cell Signaling Technology antibodies used were ACC (#3662), phospho-ACC S79 (#3661), AMPK (#2532), phospho-AMPK T172 (#2535), Atg13 (#13273), GAPDH (#5174), GFP XP (#2956), Myc tag (#2278), Parkin (#2132), Parkin monoclonal (#4211), Raptor (#2280), phospho-Raptor (#2083), phospho-S6 S235/6 (#4858), TBK1 (#3013), phospho-TBK1 S172 (#5483), ULK1 (#8054), phospho-ULK1 S555 (#5869), phospho-ULK1 S757 (#6888), 4EBP1 (#9452). Phospho-Parkin Ser108 antibody was developed in

collaboration with Thorsten Wiederhold at Cell Signaling Technology. Phospho-Vps34 Ser249 antibody was developed in collaboration with Gary Kasof at Cell Signaling Technology as reported previously (Egan et al., 2015). Sigma antibodies used were ULK1 (A7481), b-actin (A5541), and Flag tag polyclonal (F7425). MitoNEET/CISD1 (16006-1-AP) antibody was from ProteinTech. Phospho-Atg13 Ser318 (600-401-C49) antibody was from Rockland. Mitofusin2 (ab124773) antibody was from Abcam. Mitochondrial electron transport chain complexes were blotted using the MitoProfile Total OXPHOS antibody cocktail (ab110413). EBSS (14155-063) was from GIBCO/Life Technologies. CCCP (C2759), Rotenone (R8875), and Phenformin (P7045) were from Sigma. INK-128 (A-1023) was from Active Bio-chem. AICAR (A611700) was from Toronto Research Chemicals.

Plasmids

YFP-Parkin plasmid (#23955) was from Addgene. The cDNA encoding human Vps34 was obtained from Invitrogen. The Flag tag and attL1 sites (for BP reaction) were cloned by PCR using standard methods. cDNAs were subcloned into pDONR221 with BP clonase (Invitrogen), and site-directed mutagenesis was performed using QuikChange II XL (Stratagene). Kinase dead ULK1 was achieved by introduction of a K46I mutation. Wild-type and mutant alleles in pDONR221 were sequenced in their entirety to verify no additional mutations were introduced during PCR or mutagenesis steps and

then put into either pcDNA3 Myc or pcDNA3 Flag mammalian expression vectors, or pQCXIN retroviral destination vector (#17399) from Addgene by LR reaction (Invitrogen).

Cell Culture, Transient Transfections, and Cell Lysis

HEK-293T and SV40 immortalized wild-type mouse embryonic fibroblast (MEF) cells were cultured in DMEM (Mediatech) containing 10% fetal bovine serum (Hyclone, Thermo Scientific) and penicillin/streptomycin (Gibco) at 37°C in 10% CO2. For transient expression, cells were transfected with 2 µg each DNA plasmid per 6 cm dish using Lipofectamine 2000 (Invitrogen) following the manufacturer's protocol. Cells were harvested 16 hours after transfection in Cell Signaling Technology lysis buffer supplemented with EDTA-free protease inhibitor cocktail (11836170001) from Roche and Calyculin A (1336100U) from Tocris. Cell lysates were prepared and immunoblotted as previously described (Egan et al., 2011). siRNA transfections were performed using ON-TARGETplus SMARTpools from Dharmacon transfected at a final concentration of 20 nM using RNAiMAX (Invitrogen) according to the manufacturer’s protocol, and cell lysates were harvested 72 hours after transfection. Immunoprecipitations were performed by incubating the cell lysates at 4°C for 2 hours with the indicated antibodies and Protein A- or G-Sepharose 4B Conjugate (for rabbit or mouse antibodies, respectively) from Invitrogen or by incubation with GFP-Trap (Bulldog Bio)

where indicated. Phosphatase treatment was performed using lambda protein phosphatase (P0753S) from New England BioLabs.

Generation of YFP-Parkin MEFs, and Fluorescence Microscopy

Stable retroviral expression of wildtype and mutant YFP-Parkin in MEF cells was performed as described previously (3). Briefly, the pQCXIN YFP-Parkin constructs were transfected along with the ampho packaging plasmid into HEK293T cells, the virus-containing supernatants were collected 48 hours after transfection and passed through 0.45 um filters, and target MEFs were infected in the presence of polybrene (5 ug/ml; Sigma 107689). 24 hours after infection, cells were selected with neomycin (0.5 mg/ml; Invitrogen 10131027). MEFs stably expressing YFP-Parkin were plated on glass coverslips in 6-well tissue culture plates. 16 hours later, cells were treated as indicated and subsequently fixed in 4% PFA (Electron Microscopy Sciences) in PBS for 10 minutes and permeabilized in 0.2% Triton in PBS for 10 minutes. Mitochondria were stained using the primary antibody Tom20 (1:200; Santa Cruz sc-11415) and secondary antibody anti-rabbit AlexaFluor 555 (1:1000; Molecular Probes), and counter stained with DAPI (Sigma). Coverslips were mounted in Fluoromount-G (SouthernBiotech). Images were acquired on a Zeiss LSM 700 confocal microscope, and scoring was performed blind to cellular genotype/expression and treatment.

Mass Spectrometry

YFP-Parkin was overexpressed in HEK-293T cells as described and immunoprecipitated with GFP-Trap (Bulldog Bio), run out on SDS-PAGE gels, and stained with GelCode blue reagent (Thermo Scientific). Bands on the gels were cut out and subjected to reduction with dithiothreitol, alkylation with iodoacetamide, and in-gel digestion with trypsin or chymotrypsin overnight at pH 8.3, followed by reversed-phase microcapillary/tandem mass spectrometry (LC/MS/MS). LC/MS/MS was performed using an Easy-nLC nanoflow HPLC (Proxeon Biosciences) with a selfpacked 75 μm id x 15 cm C18 column coupled to a LTQ-Orbitrap XL mass spectrometer (Thermo Scientific) in the data-dependent acquisition and positive ion mode at 300 nL/min. Peptide ions from predicted phosphorylation sites were also targeted in MS/MS mode for quantitative analyses. MS/MS spectra collected via collision induced dissociation in the ion trap were searched against the concatenated target and decoy (reversed) single entry and full Swiss-Prot protein databases using Sequest (Proteomics Browser Software, Thermo Scientific) with differential modifications for Ser/Thr/Tyr phosphorylation (+79.97) and the sample processing artifacts Met oxidation (+15.99), deamidation of Asn and Gln (+0.984) and Cys alkylation (+57.02). Phosphorylated and unphosphorylated peptide sequences were identified if they initially passed the following Sequest scoring thresholds against the target database: 1+ ions, Xcorr ≥ 2.0 Sf ≥ 0.4, P ≥ 5; 2+ ions, Xcorr ≥ 2.0, Sf ≥ 0.4, P ≥ 5; 3+ ions, Xcorr ≥ 2.60, Sf ≥ 0.4, P ≥ 5

against the target protein database. Passing MS/MS spectra were manually inspected to be sure that all b- and y- fragment ions aligned with the assigned sequence and modification sites. Determination of the exact sites of phosphorylation was aided using FuzzyIons and GraphMod and phosphorylation site maps were created using ProteinReport software (Proteomics Browser Software suite, Thermo Scientific). False discovery rates (FDR) of peptide hits (phosphorylated and unphosphorylated) were estimated below 1.5% based on reversed database hits.

Generation and sequencing of CRISPR cell lines

CRISPR knockout cell lines were generated using the Cas9 nickase strategy as described previously (71). Briefly, a guide RNA (gRNA) pair was designed to target each of the indicated human genes (ULK1, ULK2, or TBK1) using the online design tool at crispr.mit.edu. Each gRNA duplex was cloned into pX462 vector encoding SpCas9n-2A-puro (Addgene # 48141). HEK293T cells were transfected with the gRNA pair using Lipofectamine 2000 (Invitrogen). 24 hours after transfection, cells were selected with puromycin (2.5 ug/ml) for 48 hours, and single cell cloning was subsequently performed by cell sorting into 96-well plates. Individual clones were screened by western blot, and selected clones were sequenced by PCR amplification and the Zero Blunt TOPO PCR cloning kit (Life Technologies) according to the manufacturer's instructions.

Clones were mini prepped and sequenced by Sanger sequencing and aligned to the reference sequence.

ACKNOWLEDGEMENTS

We would like to thank Thorsten Wiederhold (Cell Signaling Technology) for developing the phospho-S108 Parkin antibody, as well as John Asara (Harvard Medical School/Beth Israel Deaconess Medical Center) for performing the mass spectrometry analysis. The study was designed by P.S.L and R.J.S. P.S.L. was supported by the National Institute of Health (NIH) Cell & Molecular Genetics Training Program (Grant: 5T32GM007240-35) and the Chapman Charitable Trust.

Chapter Two, in part, is currently being prepared for submission for publication of the material. Lombardo, Portia S.; Hellberg, Kristina; Garcia, Daniel; Brun, Sonja N.; Shaw, Reuben J. Portia S. Lombardo was the primary investigator and author of this paper.

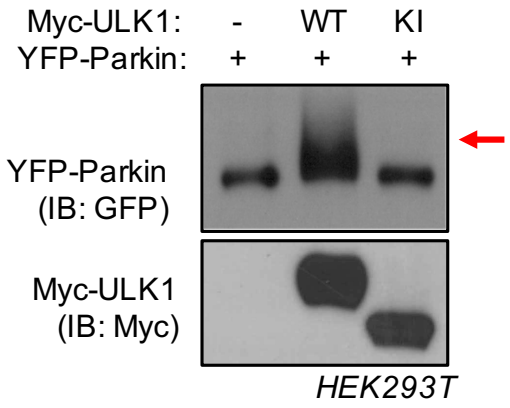

Figure 2.1A. ULK1-induced electrophoretic mobility shift of Parkin

Myc-tagged wildtype ULK1 (WT) or Myc-tagged kinase-inactive ULK1 (KI) was transfected into HEK293T cells along with wildtype YFP-tagged Parkin (YFP-Parkin). Negative control (-) for cDNA transfection was pEBG empty backbone GST fusion vector. Cellular lysates were isolated 16-hr post transfection and run on standard SDS-PAGE gels which were transferred to PVDF membranes and subsequently immunoblotted with the indicated antibodies. Red arrow indicates a mobility shift representative of phosphorylation that only occurs with the YFP-Parkin and WT ULK1 combination.

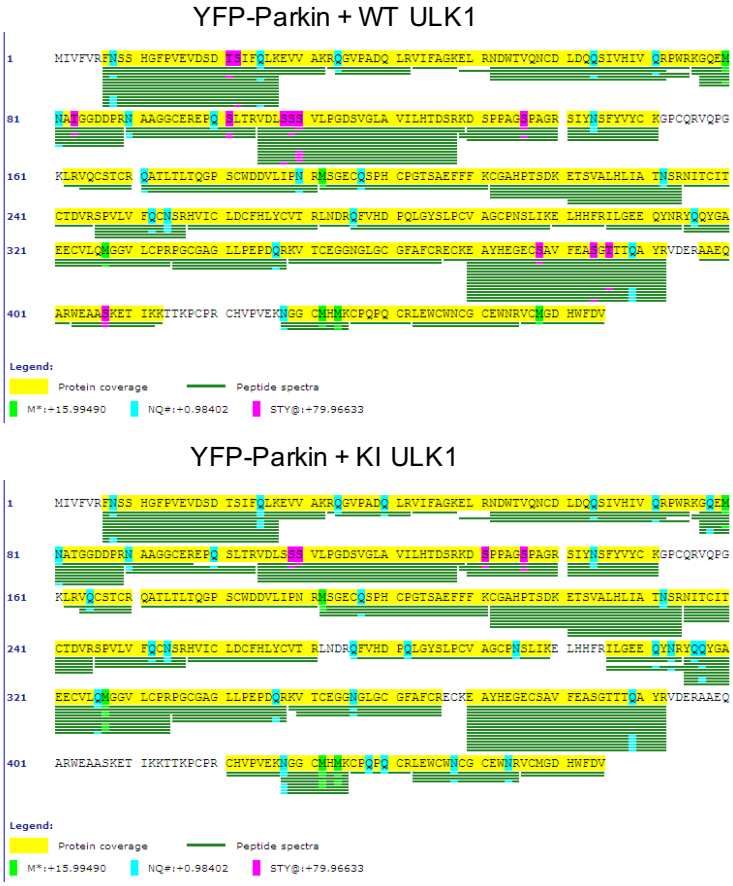

Figure 2.1B. Mass spectrometry of YFP-Parkin

WT (top) and KI (bottom) Myc-ULK1 was transfected into HEK293T cells along with YFP-Parkin. Cellular lysates were collected 16 hrs post transfection, and YFP-Parkin was immunoprecipitated with GFP-Trap conjugated agarose beads. The immunoprecipitate was run out on an SDS-PAGE gel and stained with coomassie, and the band corresponding to YFP-Parkin was isolated and subjected to tryptic digest and LC/MS/MS analysis. Green bars indicate peptide coverage, and purple highlights indicate phosphorylation events.

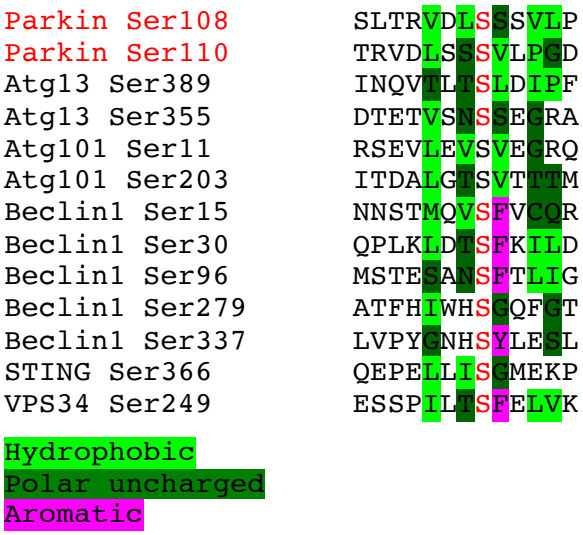

Figure 2.1C. Alignment of phosphorylation motifs of ULK1 substrates

Alignment of Parkin Ser108 and Ser110 phosphorylation sites alongside previously reported ULK1-mediated phosphorylation sites in Atg13, Atg101, Beclin1, STING, and VPS34. Residues conforming to the optimal ULK1 phosphorylation motif at the -3, -1, +1, +3 and +4 positions are highlighted.

.

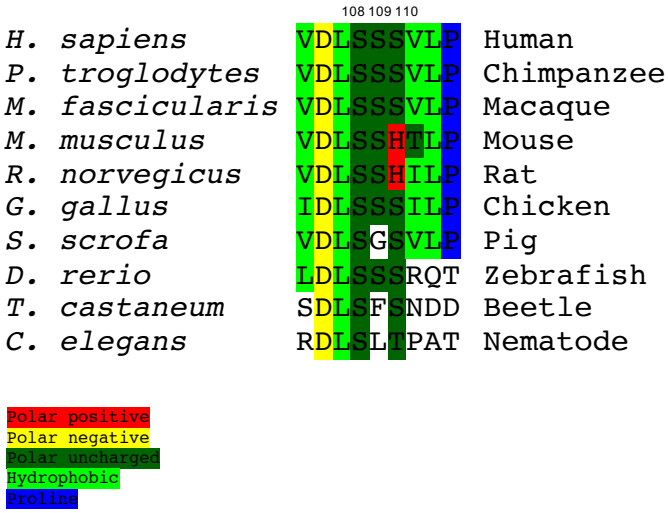

Figure 2.1D. Conservation of Parkin sites across species

The phosphoacceptor residues of Parkin S108-110 are conserved throughout evolution. Conserved residues across multiple species were aligned using NCBI Standard Protein BLAST.

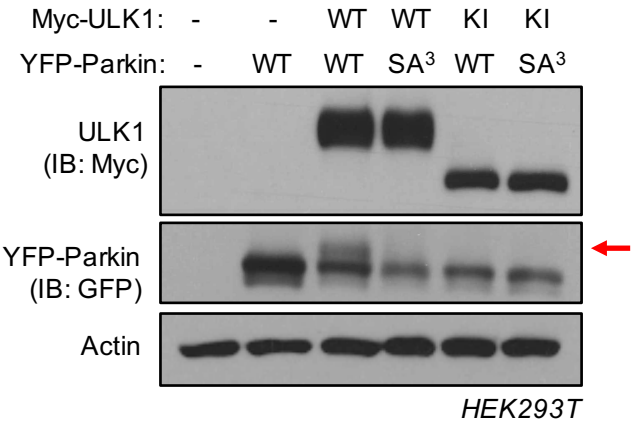

Figure 2.1E. The ULK1-induced bandshift is ablated by mutation of S108-110

WT or KI Myc-ULK1 was transfected into HEK293T cells along with wildtype (WT) or S108-110A (SA^3) YFP-Parkin. Cellular lysates were isolated 16-hr post transfection, run on standard SDS-PAGE gels which were transferred to PVDF membranes and subsequently immunoblotted with the indicated antibodies. Red arrow indicates a mobility shift representative of phosphorylation that only occurs with the WT YFP-Parkin and WT ULK1 combination.

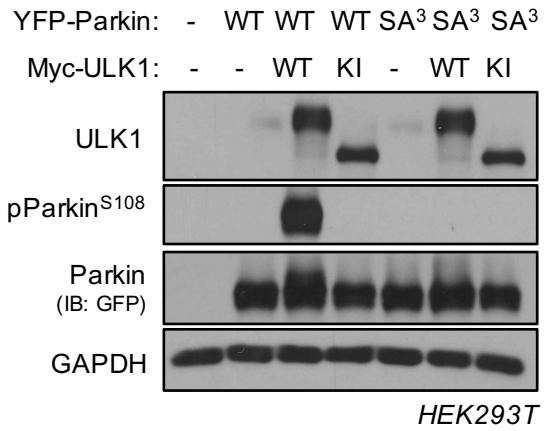

Figure 2.2A. A novel phospho-antibody detects ULK1 kinase-dependent phosphorylation of Parkin S108-110

WT or KI Myc-ULK1 was transfected into HEK293T cells along with WT or SA^3 YFP-Parkin. Cellular lysates were isolated 16-hr post transfection and subsequently immunoblotted with the indicated antibodies, including a novel phospho-specific Parkin antibody ($pParkin^{S108}$).

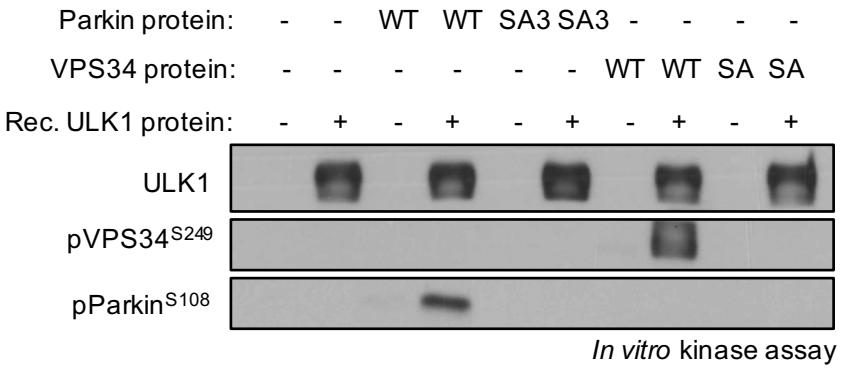

Figure 2.2B. Parkin S108-110 is phosphorylated *in vitro* by ULK1

An *in vitro* kinase assay was performed using either Parkin or VPS34 as substrates for recombinant (Rec.) ULK1 in the presence of ATP. Parkin and VPS34 were isolated by transfection of wildtype Myc-Parkin or Flag-VPS34 into HEK293T cells and subsequent immunoprecipitation 16-h post transfection using monoclonal antibodies directed toward the epitope tag (anti-Myc and anti-Flag, respectively) and sepharose beads conjugated to recombinant Protein G. *In vitro* kinase assay reactions were run on a standard SDS-PAGE gel and subsequently immunoblotted with the indicated antibodies.

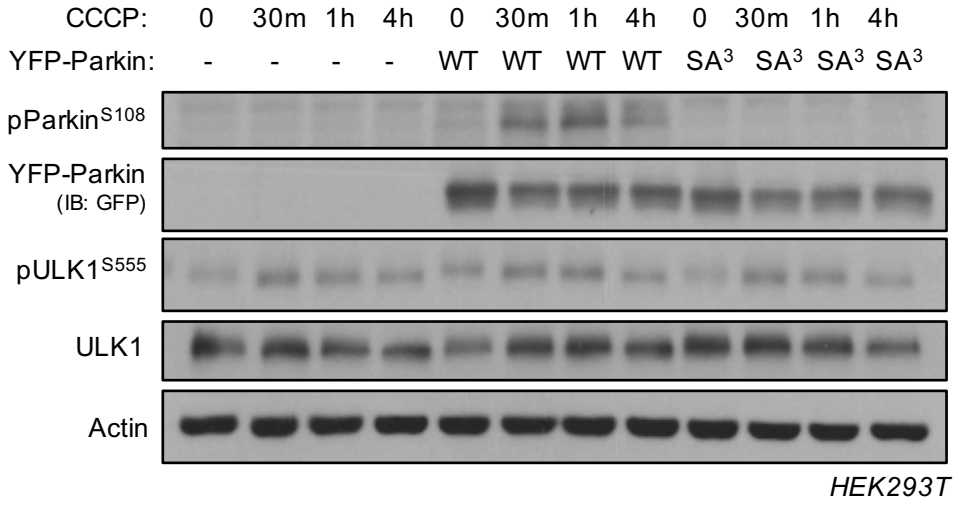

Figure 2.2C. Phosphorylation of Parkin S108-110 is induced by CCCP

WT or SA^3 YFP-Parkin was transfected into HEK293T cells. 16-h post transfection, cells were treated with 20 uM CCCP (or equivalent volume DMSO vehicle control, 0). Cellular lysates were isolated after the times indicated (30 min, 1 hour, 4 hours) and immunoblotted with the indicated antibodies.

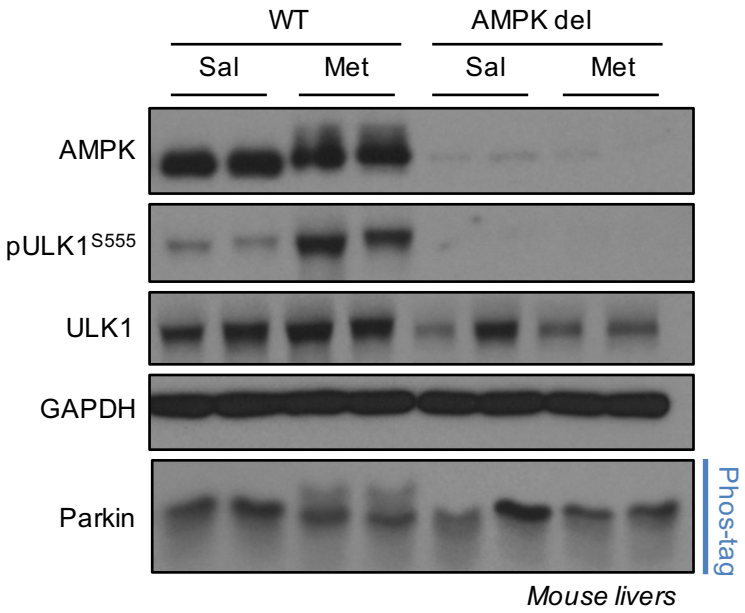

Figure 2.2D. Metformin induces phosphorylation of endogenous Parkin in an AMPK/ULK1-dependent manner in mouse liver

AMPK a1/a2 fl/fl mice expressing ("AMPK del") or not expressing ("WT") albumin-cre were treated with tamoxifen (1 mg/kg) every other day for a total of 3 injections. Mice were then fasted overnight, refed for 1 hr, then treated for 1 hr with saline or Metformin (250 mg/kg). Livers were collected, lysates were prepared in Cell Signaling Technology lysis buffer supplemented with 5X EDTA-free protease inhibitor cocktail Roche and Calyculin A, and subsequently run on standard SDS-PAGE gels or Phos-tag acrylamide gel as indicated, then immunoblotted with the indicated antibodies.

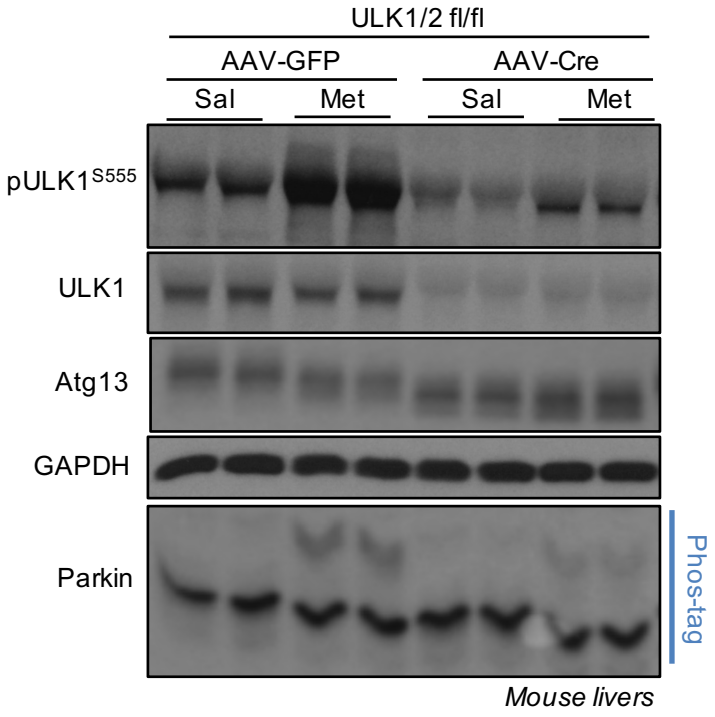

Figure 2.2E. ULK1 loss reduces Metformin-induced phosphorylation of endogenous Parkin

ULK1/2 fl/fl mice were administered AAV-GFP or AAV-Cre by tail vein injection. 2 weeks post-injection, mice were treated for 2 hrs with saline or Metformin (250 mg/kg). Livers were collected, lysates were prepared in Cell Signaling Technology lysis buffer supplemented with 5X EDTA-free protease inhibitor cocktail Roche and Calyculin A, and subsequently run on standard SDS-PAGE gels or Phos-tag acrylamide gel as indicated, then immunoblotted with the indicated antibodies.

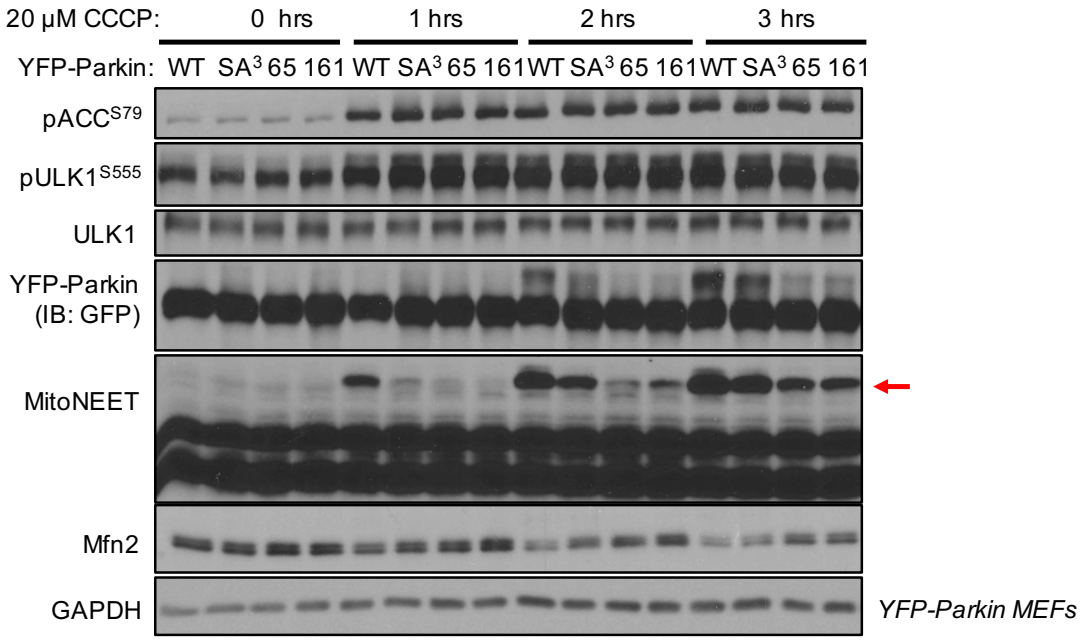

Figure 2.3A. Ubiquitination of Parkin substrates is impaired by Parkin S108-110A mutation

MEF cells stably expressing WT or mutant (S108-110A, SA^3; S65A, 65; K161N, 161) YFP-Parkin were treated with 20 uM CCCP (or equivalent volume DMSO vehicle). Cellular lysates were isolated after the times indicated and subsequently immunoblotted with the indicated antibodies. Red arrow indicates the higher molecular band of ubiquitinated MitoNEET.

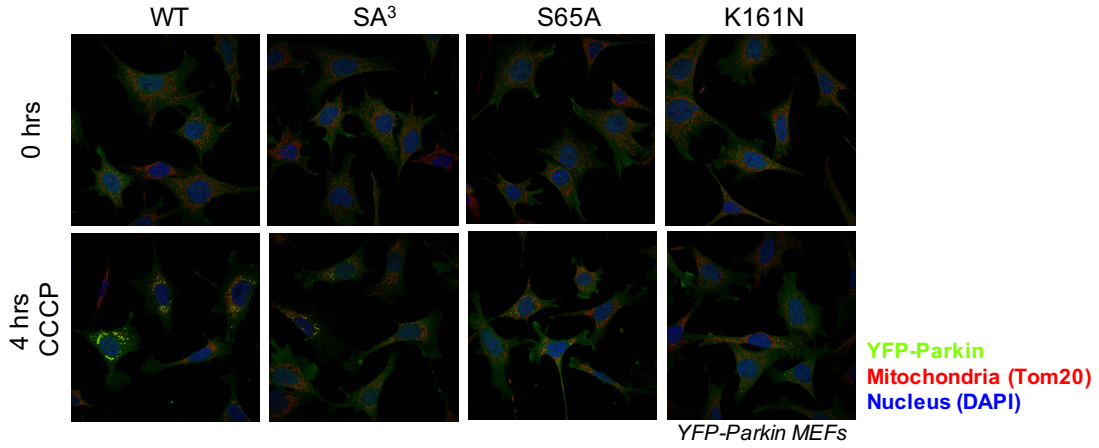

Figure 2.3B. Translocation of Parkin to damaged mitochondria is impaired by Parkin S108-110A mutation

Immunofluorescence imaging of MEF cells stably expressing WT or mutant (SA^3, S65A, K161N) YFP-Parkin, treated with 20 uM CCCP or equivalent volume DMSO vehicle control for 4 hrs. YFP-Parkin (green) was visualized by the fluorescent YFP tag, while mitochondria (red) were immunostained by the outer mitochondrial membrane protein Tom20, and nuclei (blue) were counterstained with DAPI.

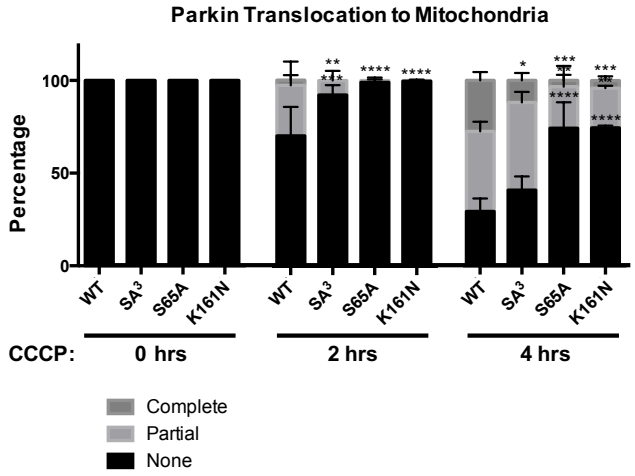

Figure 2.3C. Translocation of Parkin to damaged mitochondria is significantly delayed by Parkin S108-110A mutation

Quantification of Parkin mitochondrial translocation phenotype described in (B). MEF cells stably expressing WT or mutant (SA^3, S65A, K161N) YFP-Parkin were treated with 20 uM CCCP or equivalent volume DMSO vehicle control for the times indicated prior to fixation and immunofluorescence staining (mitochondria: Tom20; nuclei: DAPI). Data are shown as the mean ± SEM of three independent experiments with ≥100 cells counted for each condition for each replicate. *P<0.01-0.05; **P<0.001-0.01; ***P<.0001-.001; ****P<.0001by two- way analysis of variance (ANOVA).

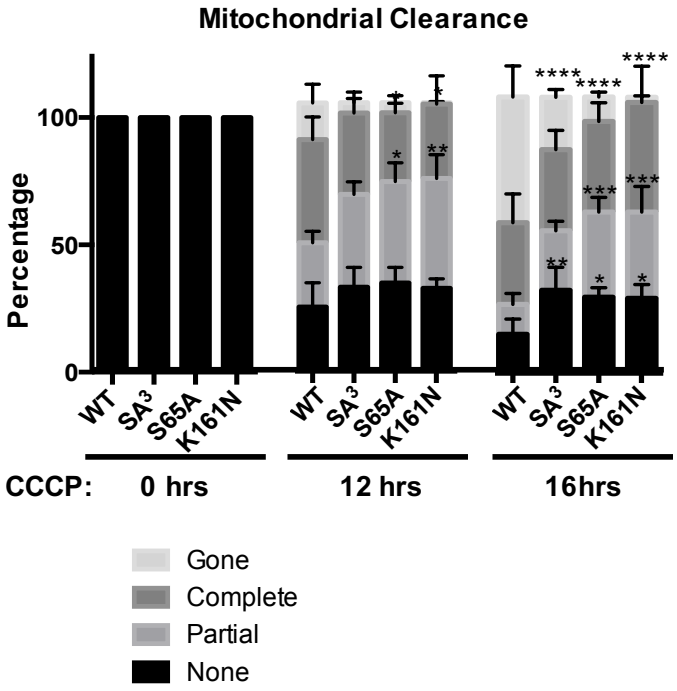

Figure 2.3D. Clearance of damaged mitochondria is delayed by Parkin S108-110A mutation

Quantification of Parkin mitochondrial clearance phenotype by immunofluorescence. MEF cells stably expressing WT or mutant (SA^3, S65A, K161N) YFP-Parkin were treated with 20 uM CCCP or equivalent volume DMSO vehicle control for the times indicated prior to fixation and immunofluorescence staining (mitochondria: Tom20; nuclei: DAPI). Data and statistics were collected as in (3C).

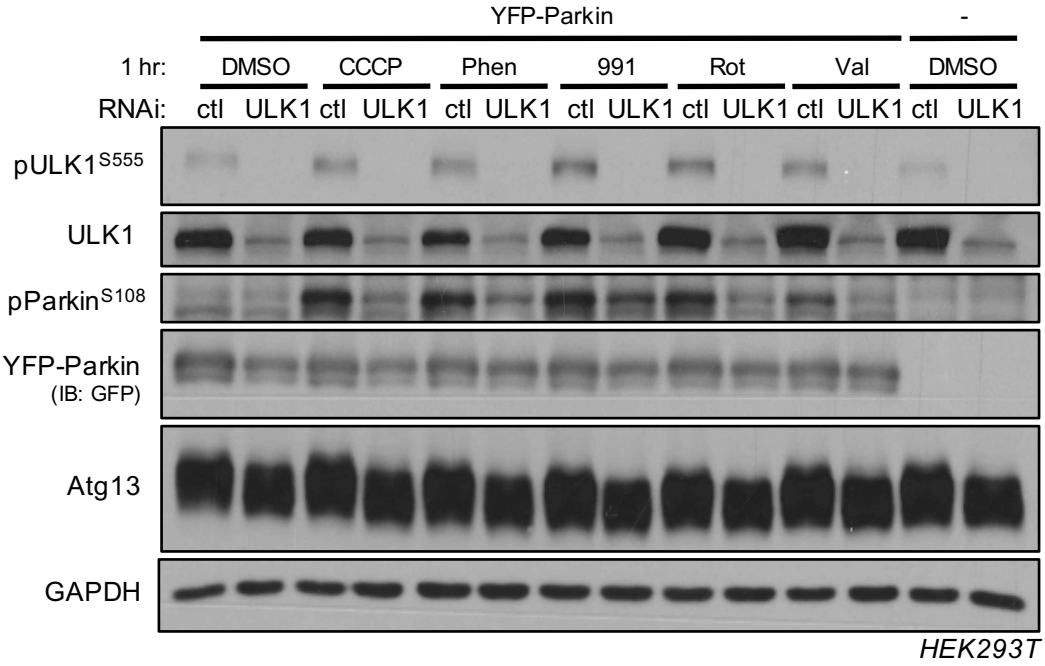

Figure 2.4A. ULK1 knockdown ablates the AMPK/ULK1 activator-induced phosphorylation of Parkin S108-110

RNAi knockdown of ULK1 (or scramble RNAi control, ctl) was performed in HEK293T cells for 72 hrs. Cells were transfected with YFP-Parkin 16 hrs prior to collection. 1 hr prior to collection, cells were treated with 20 uM CCCP, 2 mM Phenformin (Phen), 10 uM 991, 100 ng/ml Rotenone (Rot), 10 uM Valinomycin (Val), or equivalent volume vehicle control (DMSO). Cellular lysates were isolated and subsequently immunoblotted with the indicated antibodies.

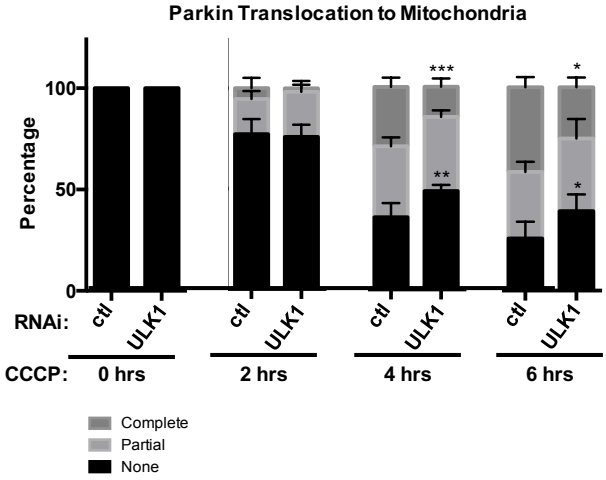

Figure 2.4B. ULK1 knockdown delays translocation of Parkin to damaged mitochondria

Quantification of Parkin mitochondrial translocation phenotype. MEF cells stably expressing WT YFP-Parkin were treated for 72 hrs with RNAi knockdown of ULK1 or scramble control (ctl). Prior to fixation and immunofluorescence staining (mitochondria: Tom20; nuclei: DAPI), cells were treated with 20 uM CCCP or equivalent volume DMSO vehicle control for the times indicated. Data are shown as the mean ± SEM of three independent experiments with ≥100 cells counted for each condition for each replicate. *P<0.01-0.05; **P<0.001-0.01; ***P<.0001-.001; ****P<.0001by two- way analysis of variance (ANOVA).

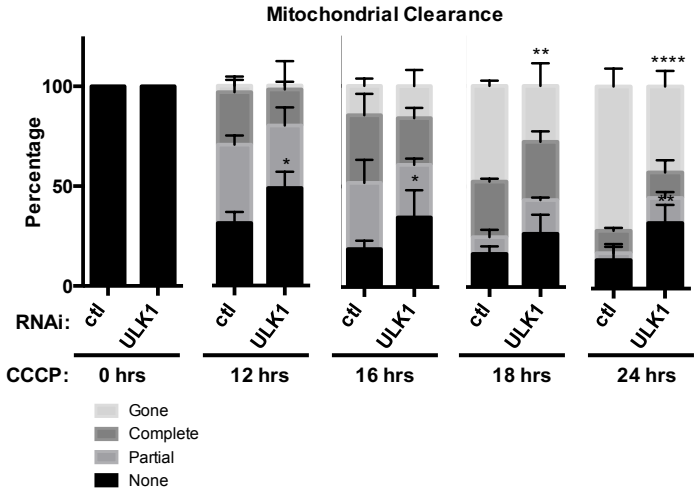

Figure 2.4C. ULK1 knockdown impairs clearance of damaged mitochondria

Quantification of Parkin mitochondrial clearance phenotype. MEF cells stably expressing WT YFP-Parkin were treated for 72 hrs with RNAi knockdown of ULK1 or scramble control (ctl). Prior to fixation and immunofluorescence staining (mitochondria: Tom20; nuclei: DAPI), cells were treated with 20 uM CCCP or equivalent volume DMSO vehicle control for the times indicated. Data and statistics were collected as in (4B).

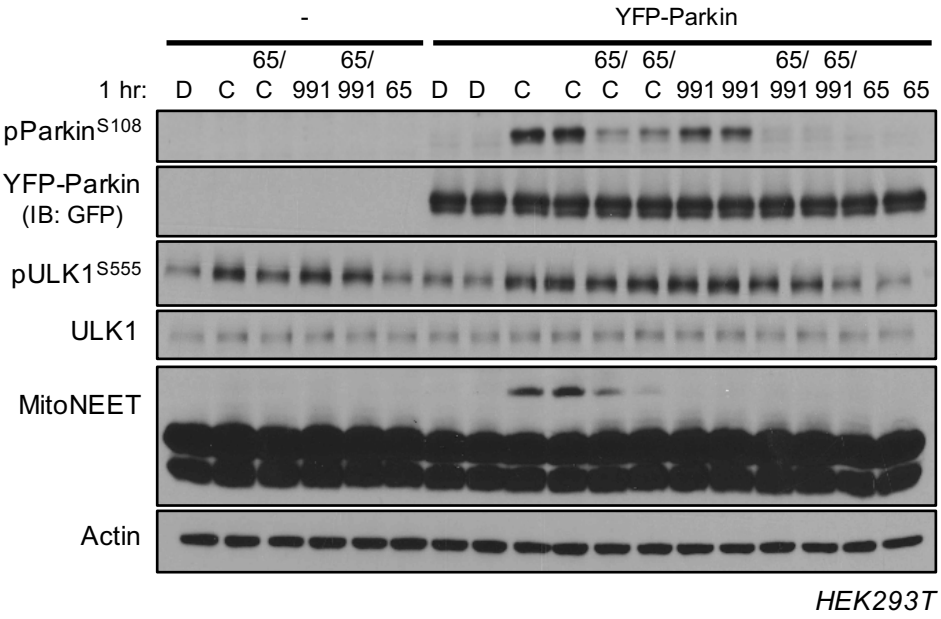

Figure 2.4D. Inhibition of ULK1 ablates the CCCP- and 991-induced phosphorylation of Parkin S108-110

YFP-Parkin was transfected into HEK293T cells. 16 hrs post transfection, cells were treated with DMSO vehicle control (D), 20 uM CCCP (C), 10 uM 991, 10 uM 6965 ULK1 inhibitor (65), or combination of 6965 with CCCP or 991 (65/C, 65/991, respectively) for 1 hr. Cellular lysates were isolated and subsequently immunoblotted with the indicated antibodies.

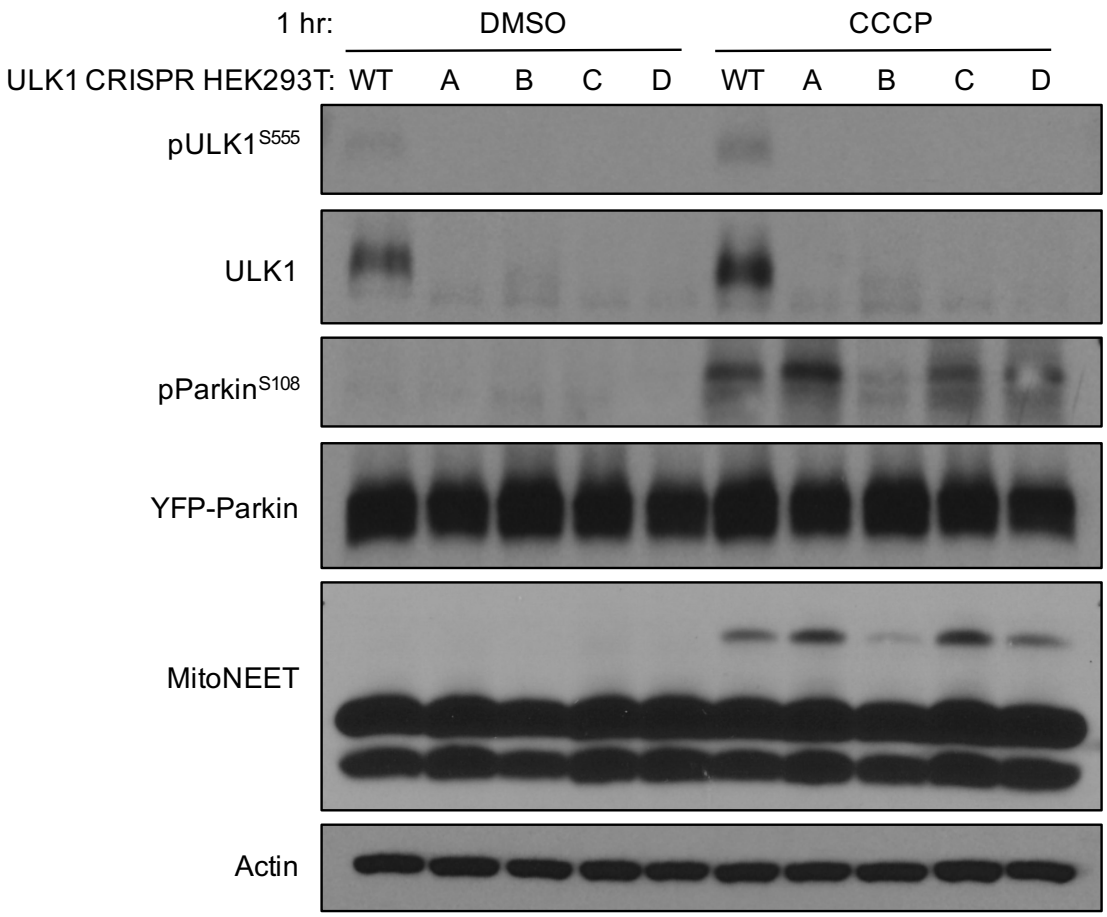

Figure 2.5A. ULK1 knockout CRISPR clones display compensatory phosphorylation of Parkin S108-110

WT HEK293T cells (WT) and representative ULK1 knockout CRISPR clones (A-D) were treated with DMSO vehicle control or 20 uM CCCP for 1 hr. Cellular lysates were isolated and subsequently immunoblotted with the indicated antibodies.

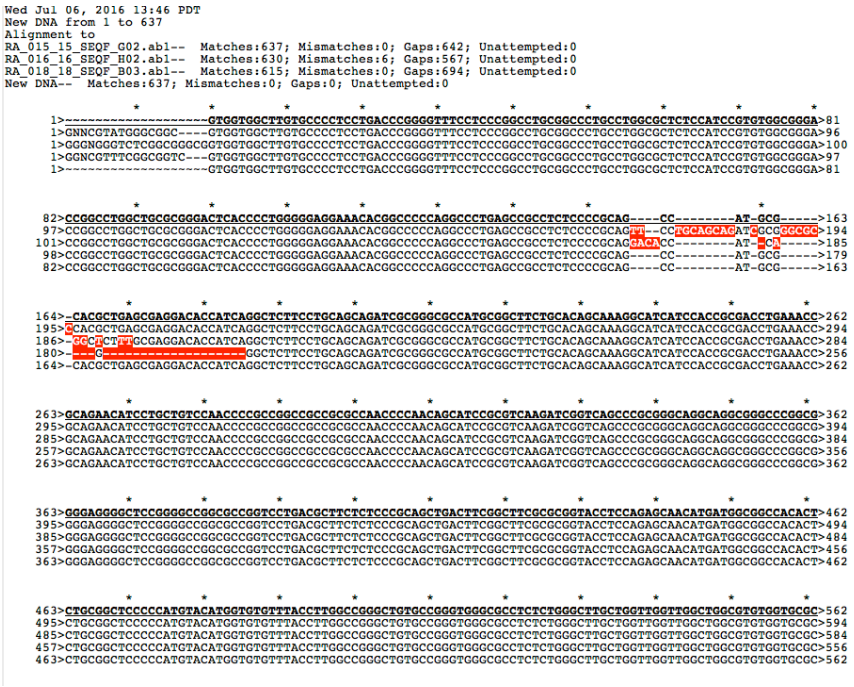

Figure 2.5B. Sequencing of ULK1 knockout CRISPR clone B

ULK1 allele sequencing of HEK293T CRISPR clone B was performed on TOPO cloning products and analyzed using the ApE plasmid editor.

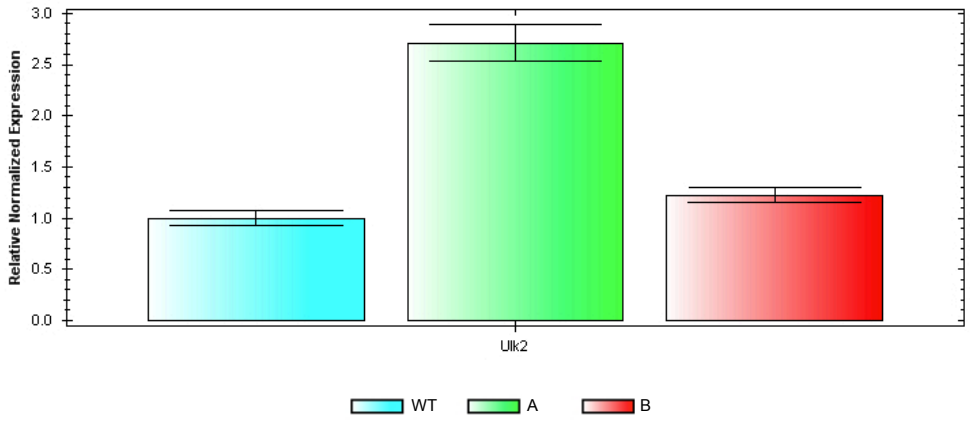

Figure 2.5C. Upregulation of ULK2 expression compensates for ULK1 loss in ULK1 knockout CRISPR clone A

qPCR analysis for ULK2 mRNA expression in WT HEK293T and ULK1 knockout CRISPR clones A and B. Values are expressed as mean ± SEM.

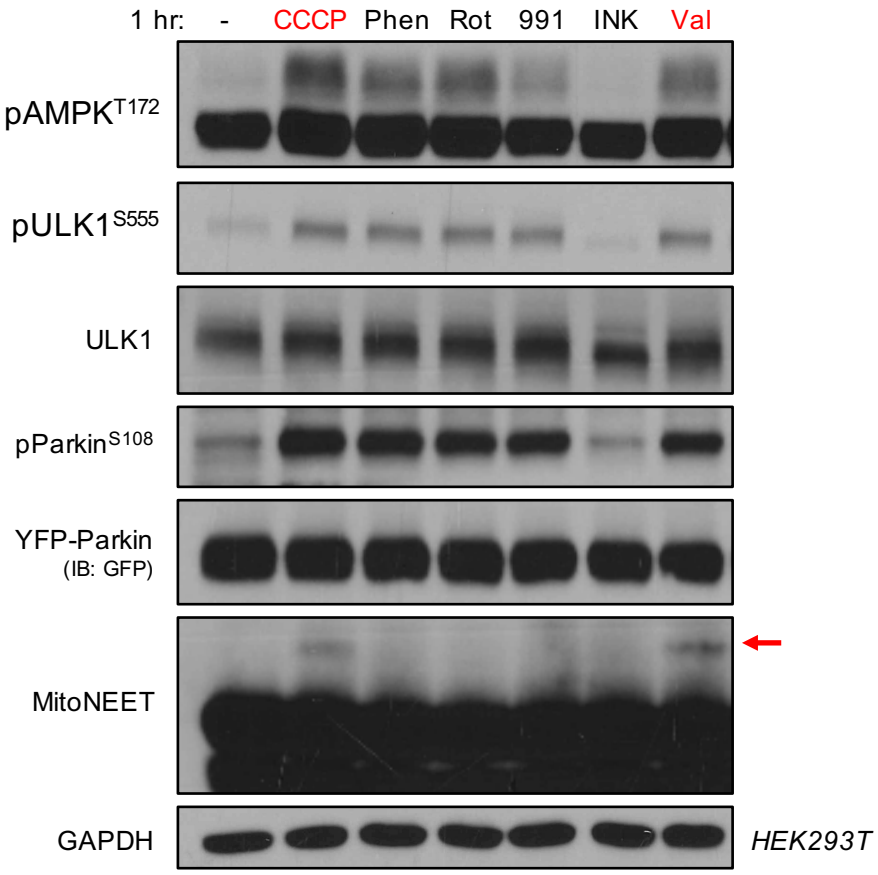

Figure 2.6A. Phosphorylation of Parkin S108-110 is not sufficient to induce ubiquitination of Parkin substrates in the absence of mitochondrial depolarization

YFP-Parkin was transfected into HEK293T cells. 16 hrs post transfection, cells were treated for 1 hr with 20 uM CCCP, 2 mM Phenformin, 100 ng/ml Rotenone, 10 uM 991, 1uM INK128, 5 uM Valinomycin, or equivalent DMSO vehicle control. Cellular lysates were isolated and subsequently immunoblotted with the indicated antibodies. Red arrow indicates higher molecular weight band of ubiquitinated MitoNEET.

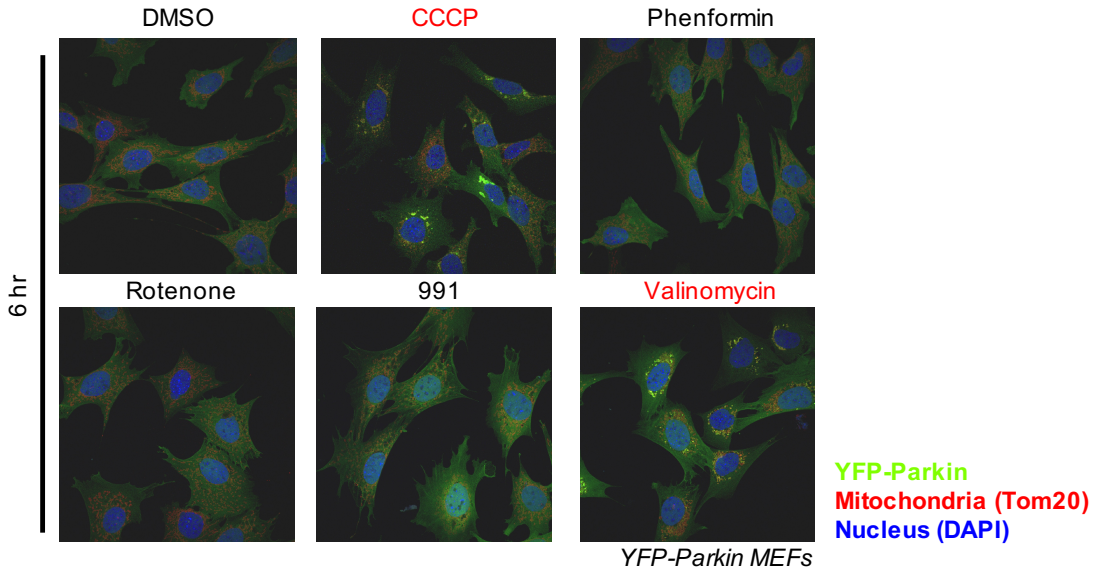

Figure 2.6B. Activation of the AMPK/ULK1 pathway is not sufficient to induce translocation of Parkin in the absence of mitochondrial depolarization

Immunofluorescence imaging of MEF cells stably expressing WT YFP-Parkin, treated 6 hrs with 20 uM CCCP, 2 mM Phenformin, 100 ng/ml Rotenone, 10 uM 991, 10 uM Valinomycin, or equivalent DMSO vehicle control. YFP-Parkin (green) was visualized by the fluorescent YFP tag, while mitochondria (red) were immunostained by the outer mitochondrial membrane protein Tom20, and nuclei (blue) were counterstained with DAPI.

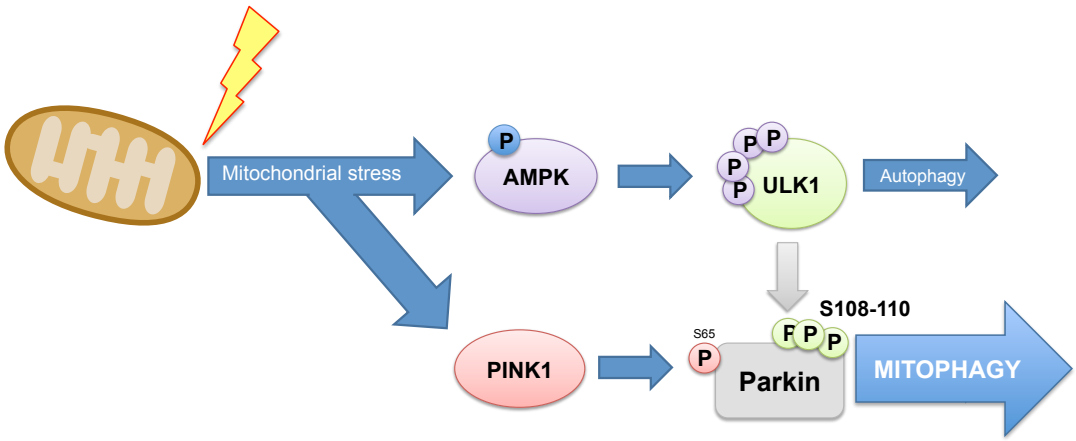

Figure 2.6C. Model

Mitochondrial stress activates the AMPK/ULK1 pathway and induces ULK1-mediated phosphorylation of Parkin at S108-110, which primes Parkin for maximal activity following mitochondrial depolarization.

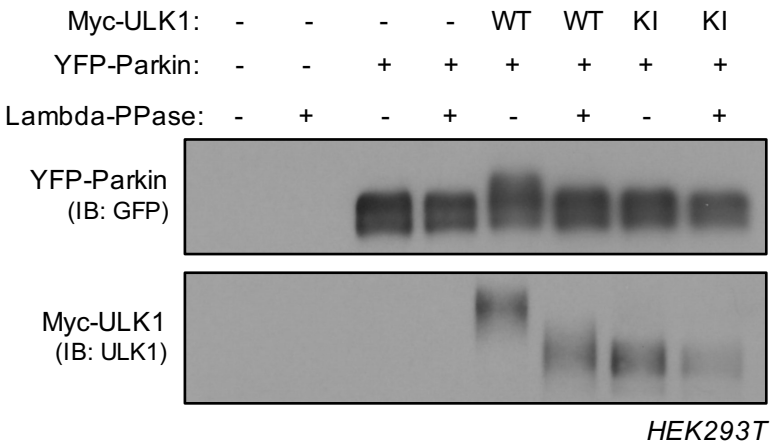

Figure 2.S1A. The ULK1-induced bandshift of Parkin is collapsible by phosphatase treatment

Myc-tagged wildtype ULK1 (WT) or Myc-tagged kinase-inactive ULK1 (KI) was transfected into HEK293T cells along with wildtype YFP-tagged Parkin. Negative control (-) for cDNA transfection was pEBG empty backbone GST fusion vector. Cellular lysates were collected 16 hrs post transfection, YFP-Parkin immunoprecipitation was performed using GFP-Trap conjugated agarose beads, and samples were subsequently treated with lambda-phosphatase (PPase) or PMP buffer negative control. Samples were run out on a standard SDS-PAGE gel and subsequently immunoblotted with the indicated antibodies.

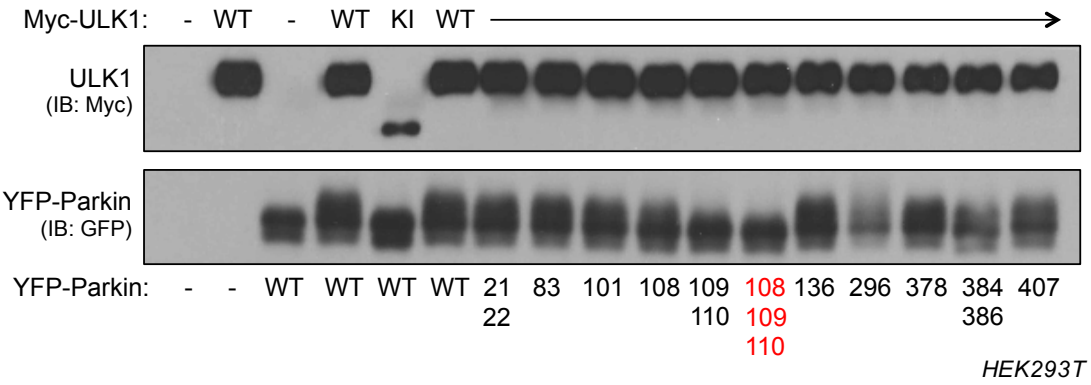

Figure 2.S1B. The ULK1-induced bandshift of Parkin is collapsible by S108-110A mutation

WT YFP-Parkin or YFP-Parkin with Ser(orThr)-to-Ala mutation of the indicated Ser/Thr residues (bottom) was transfected into HEK293T cells along with WT or KI ULK1 (top). Cellular lysates were isolated and subsequently immunoblotted with the indicated antibodies.

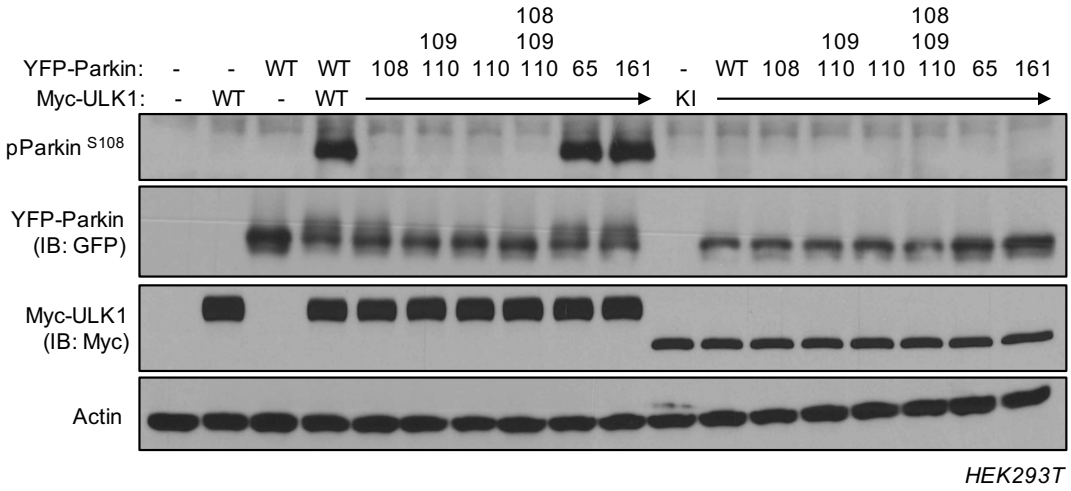

Figure 2.S2A. Phospho-antibody specificity

WT YFP-Parkin or YFP-Parkin with Ser-to-Ala mutation of the indicated Ser residues (108, 109, 110, 65) or Lys161-to-Asn mutation (161) was transfected into HEK293T cells along with WT or KI ULK1. Cellular lysates were isolated and subsequently immunoblotted with the indicated antibodies.

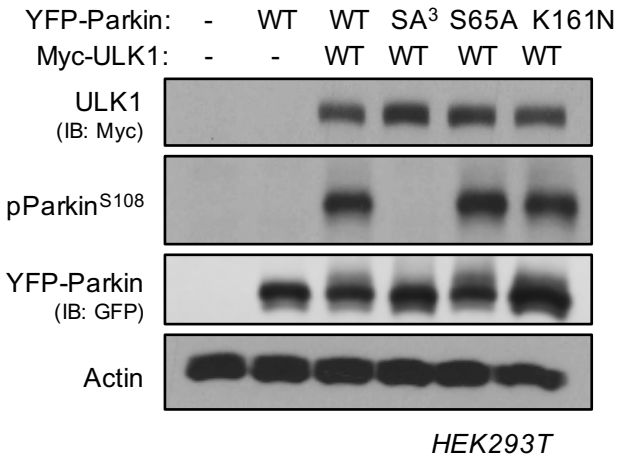

Figure 2.S2B. Phospho-Parkin S108-110 is not affected by S65A or K161N mutation

WT Myc-ULK1 was transfected into HEK293T cells along with WT or mutant (or SA^3, S65A, or K161N) YFP-Parkin. Cellular lysates were isolated 16-hr post transfection and subsequently immunoblotted with the indicated antibodies.

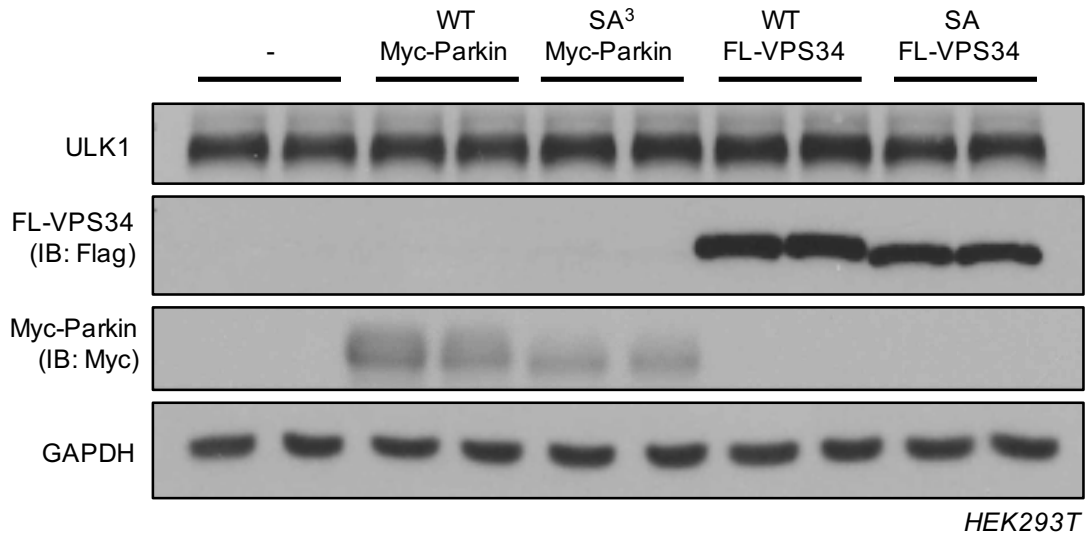

Figure 2.S2C. *In vitro* kinase assay input controls

Cellular lysates corresponding to the input controls for the *in vitro* kinase assay shown in Figure 2C. HEK293T cells were transfected with wildtype Myc-Parkin or Flag-VPS34, and cellular lysates were isolated 16-h post transfection. Input samples were collected from cellular lysates prior to immunoprecipitation described in Figure 2C. Input samples were run on a standard SDS-PAGE gel and subsequently immunoblotted with the indicated antibodies.

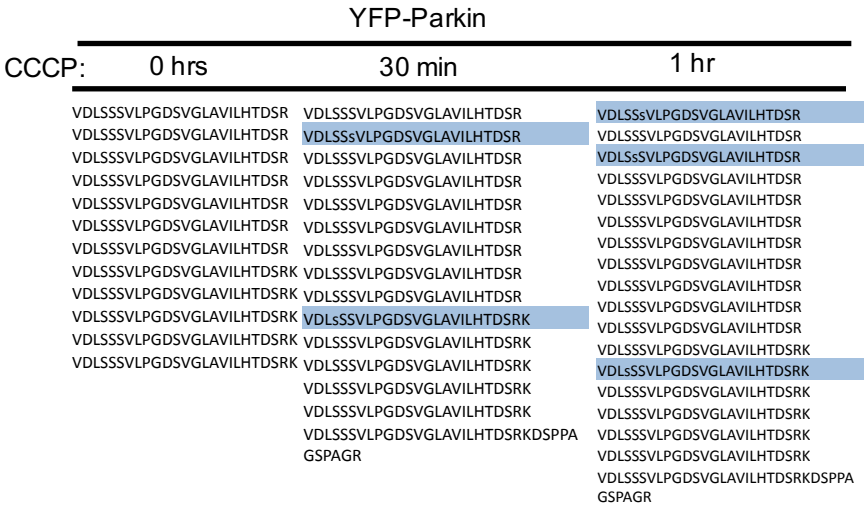

Figure 2.S2D. Mass spectrometry validation of CCCP-induced phosphorylation

Mass spectrometry coverage of peptides containing Parkin Ser108-110, with phosphorylated peptides indicated in blue (phosphorylated residue is indicated with lower case). YFP-Parkin was transfected into HEK293T cells. 16 hrs post transfection, cells were treated with 20 uM CCCP (or equivalent DMSO vehicle control) for the times indicated, then cellular lysates were collected and YFP-Parkin was immunoprecipitated with GFP-Trap conjugated agarose beads. The immunoprecipitate was run out on an SDS-PAGE gel and stained with coomassie, and the band corresponding to YFP-Parkin was isolated and subjected to tryptic digest and LC/MS/MS analysis.

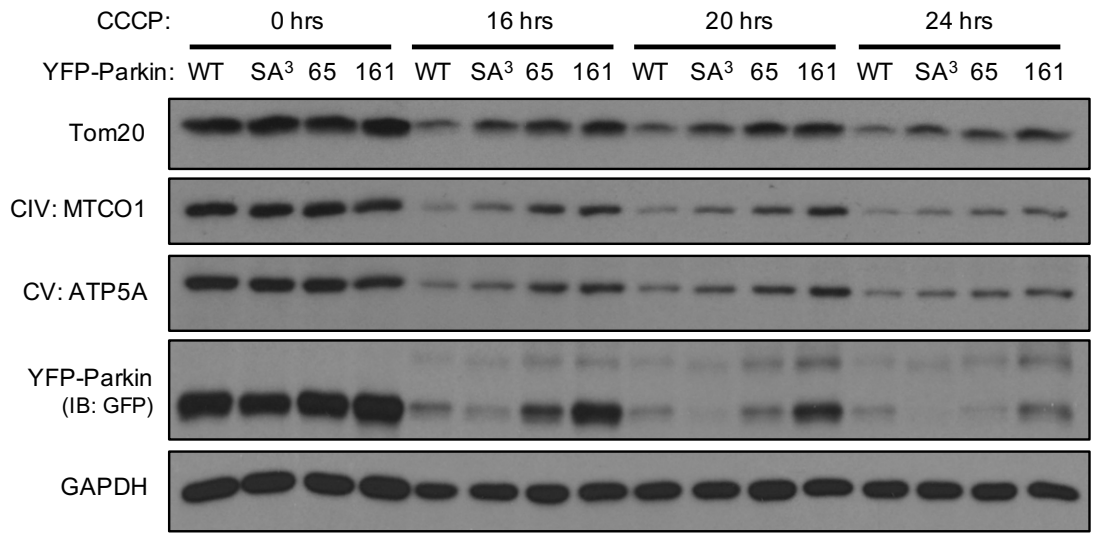

Figure 2.S3A. Parkin S108A mutation delays mitochondrial degradation

MEF cells stably expressing WT or mutant (S108-110A, SA^3; S65A, 65; K161N, 161) YFP-Parkin were treated with 20 uM CCCP (or equivalent volume DMSO vehicle control). Cellular lysates were isolated after the times indicated and subsequently immunoblotted with the indicated antibodies.

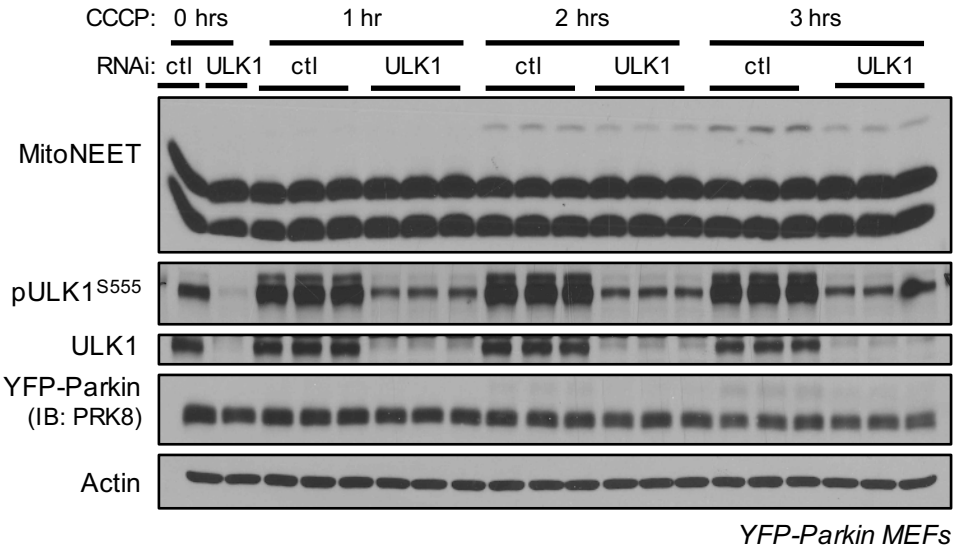

Figure 2.S4A. ULK1 knockdown impairs Parkin substrate ubiquitination

RNAi knockdown of ULK1 (or scramble RNAi control, ctl) was performed for 72 hrs in MEF cells stably expressing YFP-Parkin. Cells were treated with 20 uM CCCP or equivalent volume DMSO vehicle control for the times indicated. Cellular lysates were isolated and subsequently immunoblotted with the indicated antibodies.

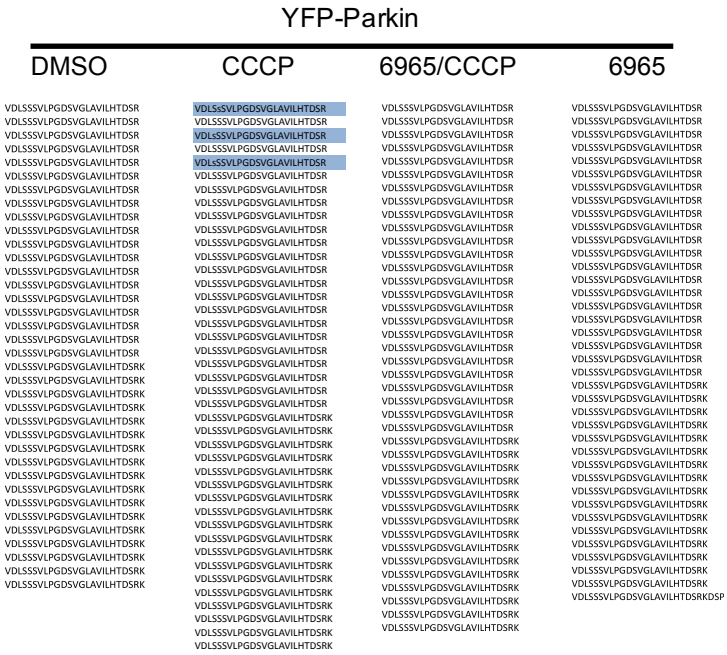

Figure 2.S4B. Small molecule inhibition of ULK1 impairs CCCP-induced phosphorylation

Mass spectrometry coverage of peptides containing Parkin Ser108-110, with phosphorylated peptides indicated in blue (phosphorylated residue is indicated with lower case). YFP-Parkin was transfected into HEK293T cells. 16 hrs post transfection, cells were treated with 20 uM CCCP, 10 uM 6965, combination (6965/CCCP), or equivalent volume DMSO vehicle control for 1 hr. Cellular lysates were collected and YFP-Parkin was immunoprecipitated with GFP-Trap conjugated agarose beads. The immunoprecipitate was run out on an SDS-PAGE gel and stained with coomassie, and the band corresponding to YFP-Parkin was isolated and subjected to tryptic digest and LC/MS/MS analysis.

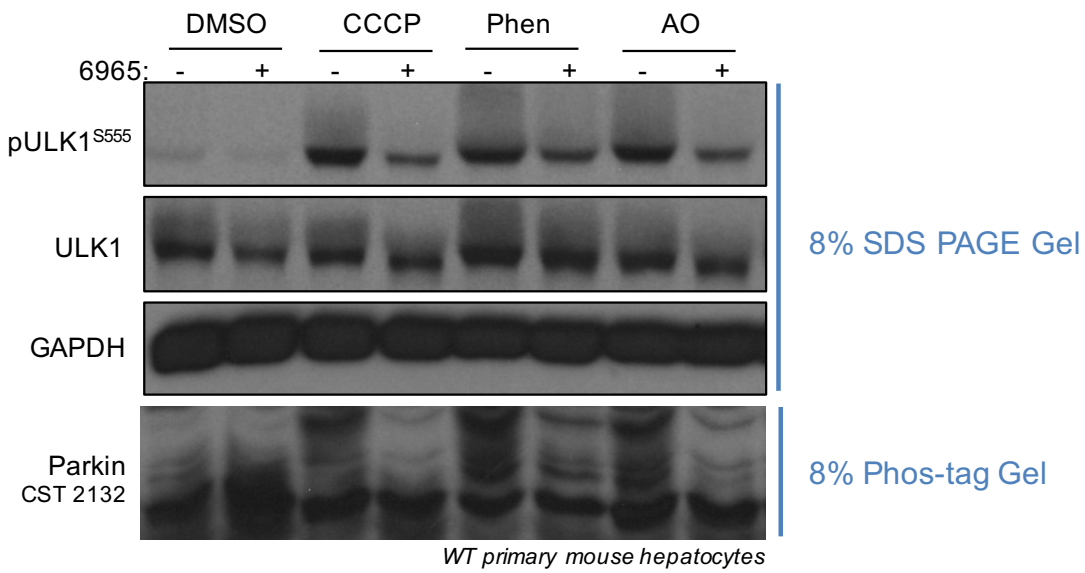

Figure 2.S4C. Phosphorylation of endogenous Parkin is ablated by co-treatment with the ULK1 inhibitor 6965

Primary hepatocytes were generated from wildtype mice, and subsequently pre-treated for 30 minutes with the ULK1 inhibitor 6965 (or equivalent DMSO), followed by co-treatment with CCCP (20 uM), Phenformin (2 mM), or a combination of antimycin and oligomycin (AO; 10 uM/5 uM), or equivalent DMSO. Cellular lysates were isolated and subsequently run on standard SDS-PAGE gels or Phos-tag acrylamide gel as indicated, then immunoblotted with the indicated antibodies.

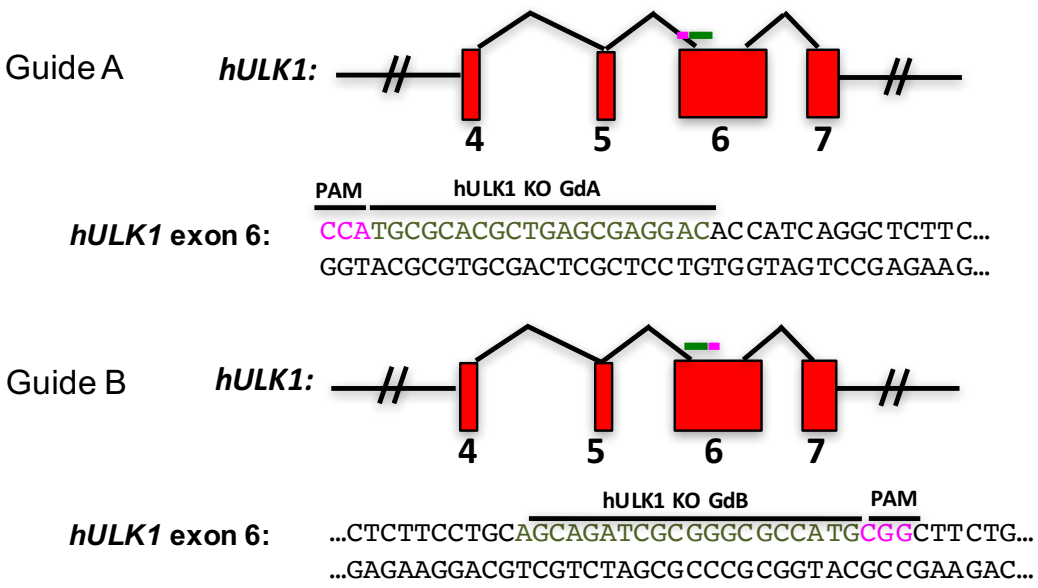

Figure 2.S5A. Human ULK1 knockout CRISPR guides

Schematic showing the relevant genomic regions and nucleotide sequences around Cas9 target sites designed for human ULK1. PAM sequences are indicated in pink, and locus-specific sgRNA sequences are indicated in green.

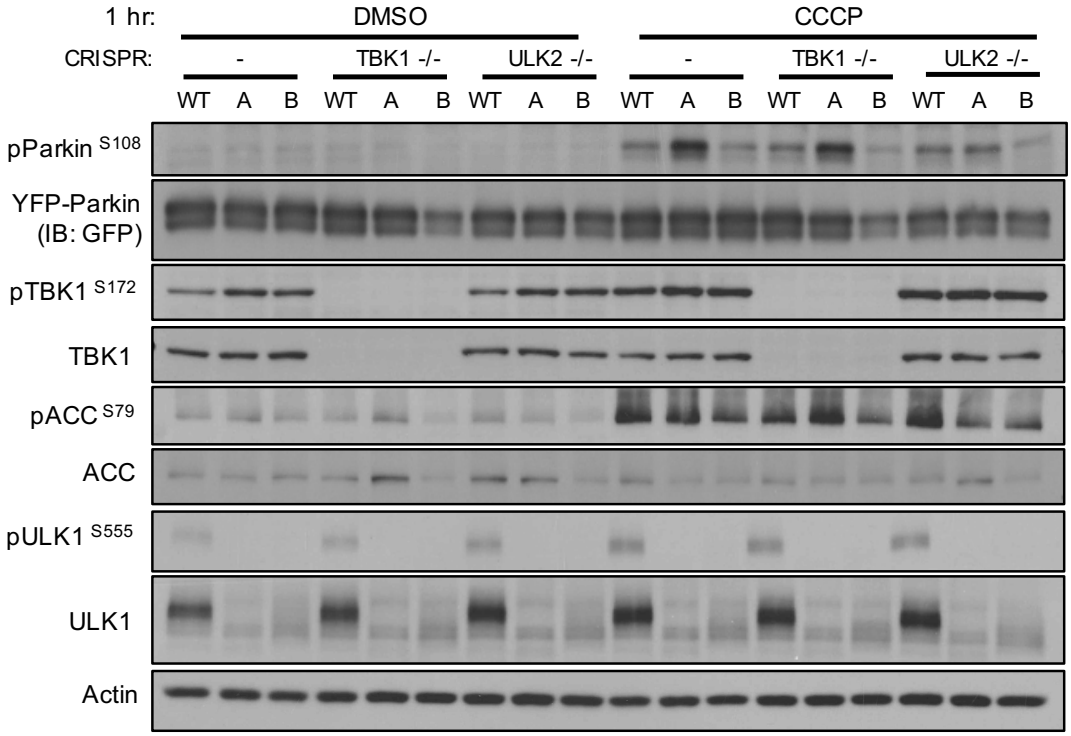

Figure 2.S5B. ULK2 knockout ablates compensatory phosphorylation of Parkin S108-110 in ULK1 knockout CRISPR clone A

WT HEK293T cells or representative ULK1 knockout CRISPR clones (A and B) were transfected with CRISPR guides targeting TBK1 or ULK2. Following selection, the polyclonal population was treated for 1 hr with 20 uM CCCP or equivalent volume DMSO vehicle control, cellular lysates were isolated and subsequently immunoblotted with the indicated antibodies.

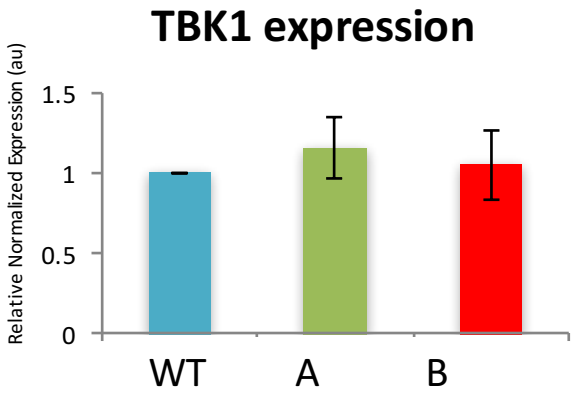

Figure 2.S5C. TBK1 expression is not affected

qPCR analysis for TBK1 mRNA expression in WT HEK293T and ULK1 knockout CRISPR clones A and B. Values are expressed as mean ± SEM.

REFERENCES

1. Manning G, Whyte DB, Martinez R, Hunter T, Sudarsanam S. The protein kinase complement of the human genome. Science. 2002;298(5600):1912-34. doi: 10.1126/science.1075762. PubMed PMID: 12471243.

2. Garcia D, Shaw RJ. AMPK: Mechanisms of Cellular Energy Sensing and Restoration of Metabolic Balance. Mol Cell. 2017;66(6):789-800. doi: 10.1016/j.molcel.2017.05.032. PubMed PMID: 28622524.

3. Gwinn DM, Shackelford DB, Egan DF, Mihaylova MM, Mery A, Vasquez DS, et al. AMPK phosphorylation of raptor mediates a metabolic checkpoint. Mol Cell. 2008;30(2):214-26. doi: 10.1016/j.molcel.2008.03.003. PubMed PMID: 18439900; PubMed Central PMCID: PMCPMC2674027.

4. Egan DF, Shackelford DB, Mihaylova MM, Gelino S, Kohnz RA, Mair W, et al. Phosphorylation of ULK1 (hATG1) by AMP-activated protein kinase connects energy sensing to mitophagy. Science. 2011;331(6016):456-61. doi: 10.1126/science.1196371. PubMed PMID: 21205641; PubMed Central PMCID: PMCPMC3030664.

5. Kim J, Kundu M, Viollet B, Guan KL. AMPK and mTOR regulate autophagy through direct phosphorylation of Ulk1. Nat Cell Biol. 2011;13(2):132-41. doi: 10.1038/ncb2152. PubMed PMID: 21258367; PubMed Central PMCID: PMCPMC3987946.

6. Hardie DG. AMPK and autophagy get connected. EMBO J. 2011;30(4):634-5. doi: 10.1038/emboj.2011.12. PubMed PMID: 21326174; PubMed Central PMCID: PMCPMC3041958.

7. Mizushima N, Komatsu M. Autophagy: renovation of cells and tissues. Cell. 2011;147(4):728-41. doi: 10.1016/j.cell.2011.10.026. PubMed PMID: 22078875.

8. Chan EY, Longatti A, McKnight NC, Tooze SA. Kinase-inactivated ULK proteins inhibit autophagy via their conserved C-terminal domains using an Atg13-independent mechanism. Mol Cell Biol. 2009;29(1):157-71. doi: 10.1128/MCB.01082-08. PubMed PMID: 18936157; PubMed Central PMCID: PMCPMC2612494.

9. Hosokawa N, Hara T, Kaizuka T, Kishi C, Takamura A, Miura Y, et al. Nutrient-dependent mTORC1 association with the ULK1-Atg13-FIP200 complex required for autophagy. Mol Biol Cell. 2009;20(7):1981-91. doi:

10.1091/mbc.E08-12-1248. PubMed PMID: 19211835; PubMed Central PMCID: PMCPMC2663915.

10. Jung CH, Jun CB, Ro SH, Kim YM, Otto NM, Cao J, et al. ULK-Atg13-FIP200 complexes mediate mTOR signaling to the autophagy machinery. Mol Biol Cell. 2009;20(7):1992-2003. doi: 10.1091/mbc.E08-12-1249. PubMed PMID: 19225151; PubMed Central PMCID: PMCPMC2663920.

11. Dorsey FC, Rose KL, Coenen S, Prater SM, Cavett V, Cleveland JL, et al. Mapping the phosphorylation sites of Ulk1. J Proteome Res. 2009;8(11):5253-63. doi: 10.1021/pr900583m. PubMed PMID: 19807128.

12. Di Bartolomeo S, Corazzari M, Nazio F, Oliverio S, Lisi G, Antonioli M, et al. The dynamic interaction of AMBRA1 with the dynein motor complex regulates mammalian autophagy. J Cell Biol. 2010;191(1):155-68. doi: 10.1083/jcb.201002100. PubMed PMID: 20921139; PubMed Central PMCID: PMCPMC2953445.

13. Rajesh S, Bago R, Odintsova E, Muratov G, Baldwin G, Sridhar P, et al. Binding to syntenin-1 protein defines a new mode of ubiquitin-based interactions regulated by phosphorylation. J Biol Chem. 2011;286(45):39606-14. doi: 10.1074/jbc.M111.262402. PubMed PMID: 21949238; PubMed Central PMCID: PMCPMC3234783.

14. Takaesu G, Kobayashi T, Yoshimura A. TGFbeta-activated kinase 1 (TAK1)-binding proteins (TAB) 2 and 3 negatively regulate autophagy. J Biochem. 2012;151(2):157-66. doi: 10.1093/jb/mvr123. PubMed PMID: 21976705.

15. Dunlop EA, Hunt DK, Acosta-Jaquez HA, Fingar DC, Tee AR. ULK1 inhibits mTORC1 signaling, promotes multisite Raptor phosphorylation and hinders substrate binding. Autophagy. 2011;7(7):737-47. PubMed PMID: 21460630; PubMed Central PMCID: PMCPMC3149699.

16. Loffler AS, Alers S, Dieterle AM, Keppeler H, Franz-Wachtel M, Kundu M, et al. Ulk1-mediated phosphorylation of AMPK constitutes a negative regulatory feedback loop. Autophagy. 2011;7(7):696-706. PubMed PMID: 21460634.

17. Russell RC, Tian Y, Yuan H, Park HW, Chang YY, Kim J, et al. ULK1 induces autophagy by phosphorylating Beclin-1 and activating VPS34 lipid kinase. Nat Cell Biol. 2013;15(7):741-50. doi: 10.1038/ncb2757. PubMed PMID: 23685627; PubMed Central PMCID: PMCPMC3885611.

18. Egan DF, Chun MG, Vamos M, Zou H, Rong J, Miller CJ, et al. Small Molecule Inhibition of the Autophagy Kinase ULK1 and Identification of ULK1 Substrates. Mol Cell. 2015;59(2):285-97. doi: 10.1016/j.molcel.2015.05.031. PubMed PMID: 26118643; PubMed Central PMCID: PMCPMC4530630.

19. Wu W, Tian W, Hu Z, Chen G, Huang L, Li W, et al. ULK1 translocates to mitochondria and phosphorylates FUNDC1 to regulate mitophagy. EMBO Rep. 2014;15(5):566-75. doi: 10.1002/embr.201438501. PubMed PMID: 24671035; PubMed Central PMCID: PMCPMC4210082.

20. Park JM, Jung CH, Seo M, Otto NM, Grunwald D, Kim KH, et al. The ULK1 complex mediates MTORC1 signaling to the autophagy initiation machinery via binding and phosphorylating ATG14. Autophagy. 2016;12(3):547-64. doi: 10.1080/15548627.2016.1140293. PubMed PMID: 27046250; PubMed Central PMCID: PMCPMC4835982.

21. Joo JH, Wang B, Frankel E, Ge L, Xu L, Iyengar R, et al. The Noncanonical Role of ULK/ATG1 in ER-to-Golgi Trafficking Is Essential for Cellular Homeostasis. Mol Cell. 2016;62(4):491-506. doi: 10.1016/j.molcel.2016.04.020. PubMed PMID: 27203176; PubMed Central PMCID: PMCPMC4993601.

22. Gan W, Zhang C, Siu KY, Satoh A, Tanner JA, Yu S. ULK1 phosphorylates Sec23A and mediates autophagy-induced inhibition of ER-to-Golgi traffic. BMC Cell Biol. 2017;18(1):22. doi: 10.1186/s12860-017-0138-8. PubMed PMID: 28486929; PubMed Central PMCID: PMCPMC5424413.

23. Mok J, Kim PM, Lam HY, Piccirillo S, Zhou X, Jeschke GR, et al. Deciphering protein kinase specificity through large-scale analysis of yeast phosphorylation site motifs. Sci Signal. 2010;3(109):ra12. doi: 10.1126/scisignal.2000482. PubMed PMID: 20159853; PubMed Central PMCID: PMCPMC2846625.

24. Papinski D, Schuschnig M, Reiter W, Wilhelm L, Barnes CA, Maiolica A, et al. Early steps in autophagy depend on direct phosphorylation of Atg9 by the Atg1 kinase. Mol Cell. 2014;53(3):471-83. doi: 10.1016/j.molcel.2013.12.011. PubMed PMID: 24440502; PubMed Central PMCID: PMCPMC3978657.

25. Obenauer JC, Cantley LC, Yaffe MB. Scansite 2.0: Proteome-wide prediction of cell signaling interactions using short sequence motifs. Nucleic Acids Res. 2003;31(13):3635-41. PubMed PMID: 12824383; PubMed Central PMCID: PMCPMC168990.

26. Hornbeck PV, Zhang B, Murray B, Kornhauser JM, Latham V, Skrzypek E. PhosphoSitePlus, 2014: mutations, PTMs and recalibrations. Nucleic Acids Res. 2015;43(Database issue):D512-20. doi: 10.1093/nar/gku1267. PubMed PMID: 25514926; PubMed Central PMCID: PMCPMC4383998.

27. Kitada T, Asakawa S, Hattori N, Matsumine H, Yamamura Y, Minoshima S, et al. Mutations in the parkin gene cause autosomal recessive juvenile parkinsonism. Nature. 1998;392(6676):605-8. doi: 10.1038/33416. PubMed PMID: 9560156.

28. Walden H, Muqit MM. Ubiquitin and Parkinson's disease through the looking glass of genetics. Biochem J. 2017;474(9):1439-51. doi: 10.1042/BCJ20160498. PubMed PMID: 28408429; PubMed Central PMCID: PMCPMC5390927.

29. McWilliams TG, Muqit MM. PINK1 and Parkin: emerging themes in mitochondrial homeostasis. Curr Opin Cell Biol. 2017;45:83-91. doi: 10.1016/j.ceb.2017.03.013. PubMed PMID: 28437683.

30. Riley JS, Tait SW. Mechanisms of mitophagy: putting the powerhouse into the doghouse. Biol Chem. 2016;397(7):617-35. doi: 10.1515/hsz-2016-0137. PubMed PMID: 27071149.

31. Nguyen TN, Padman BS, Lazarou M. Deciphering the Molecular Signals of PINK1/Parkin Mitophagy. Trends Cell Biol. 2016;26(10):733-44. doi: 10.1016/j.tcb.2016.05.008. PubMed PMID: 27291334.

32. Pickrell AM, Youle RJ. The roles of PINK1, parkin, and mitochondrial fidelity in Parkinson's disease. Neuron. 2015;85(2):257-73. doi: 10.1016/j.neuron.2014.12.007. PubMed PMID: 25611507; PubMed Central PMCID: PMCPMC4764997.

33. Ordureau A, Sarraf SA, Duda DM, Heo JM, Jedrychowski MP, Sviderskiy VO, et al. Quantitative proteomics reveal a feedforward mechanism for mitochondrial PARKIN translocation and ubiquitin chain synthesis. Mol Cell. 2014;56(3):360-75. doi: 10.1016/j.molcel.2014.09.007. PubMed PMID: 25284222; PubMed Central PMCID: PMCPMC4254048.

34. Narendra D, Tanaka A, Suen DF, Youle RJ. Parkin is recruited selectively to impaired mitochondria and promotes their autophagy. J Cell Biol. 2008;183(5):795-803. doi: 10.1083/jcb.200809125. PubMed PMID: 19029340; PubMed Central PMCID: PMCPMC2592826.

35. Geisler S, Holmstrom KM, Skujat D, Fiesel FC, Rothfuss OC, Kahle PJ, et al. PINK1/Parkin-mediated mitophagy is dependent on VDAC1 and

p62/SQSTM1. Nat Cell Biol. 2010;12(2):119-31. doi: 10.1038/ncb2012. PubMed PMID: 20098416.

36. Narendra DP, Jin SM, Tanaka A, Suen DF, Gautier CA, Shen J, et al. PINK1 is selectively stabilized on impaired mitochondria to activate Parkin. PLoS Biol. 2010;8(1):e1000298. doi: 10.1371/journal.pbio.1000298. PubMed PMID: 20126261; PubMed Central PMCID: PMCPMC2811155.

37. Kondapalli C, Kazlauskaite A, Zhang N, Woodroof HI, Campbell DG, Gourlay R, et al. PINK1 is activated by mitochondrial membrane potential depolarization and stimulates Parkin E3 ligase activity by phosphorylating Serine 65. Open Biol. 2012;2(5):120080. doi: 10.1098/rsob.120080. PubMed PMID: 22724072; PubMed Central PMCID: PMCPMC3376738.

38. Shiba-Fukushima K, Imai Y, Yoshida S, Ishihama Y, Kanao T, Sato S, et al. PINK1-mediated phosphorylation of the Parkin ubiquitin-like domain primes mitochondrial translocation of Parkin and regulates mitophagy. Sci Rep. 2012;2:1002. doi: 10.1038/srep01002. PubMed PMID: 23256036; PubMed Central PMCID: PMCPMC3525937.

39. Kane LA, Lazarou M, Fogel AI, Li Y, Yamano K, Sarraf SA, et al. PINK1 phosphorylates ubiquitin to activate Parkin E3 ubiquitin ligase activity. J Cell Biol. 2014;205(2):143-53. doi: 10.1083/jcb.201402104. PubMed PMID: 24751536; PubMed Central PMCID: PMCPMC4003245.

40. Koyano F, Okatsu K, Kosako H, Tamura Y, Go E, Kimura M, et al. Ubiquitin is phosphorylated by PINK1 to activate parkin. Nature. 2014;510(7503):162-6. doi: 10.1038/nature13392. PubMed PMID: 24784582.

41. Kazlauskaite A, Kondapalli C, Gourlay R, Campbell DG, Ritorto MS, Hofmann K, et al. Parkin is activated by PINK1-dependent phosphorylation of ubiquitin at Ser65. Biochem J. 2014;460(1):127-39. doi: 10.1042/BJ20140334. PubMed PMID: 24660806; PubMed Central PMCID: PMCPMC4000136.

42. Wauer T, Simicek M, Schubert A, Komander D. Mechanism of phospho-ubiquitin-induced PARKIN activation. Nature. 2015;524(7565):370-4. doi: 10.1038/nature14879. PubMed PMID: 26161729; PubMed Central PMCID: PMCPMC4984986.

43. Huttlin EL, Jedrychowski MP, Elias JE, Goswami T, Rad R, Beausoleil SA, et al. A tissue-specific atlas of mouse protein phosphorylation and expression. Cell. 2010;143(7):1174-89. doi: 10.1016/j.cell.2010.12.001. PubMed PMID: 21183079; PubMed Central PMCID: PMCPMC3035969.

44. Tian W, Li W, Chen Y, Yan Z, Huang X, Zhuang H, et al. Phosphorylation of ULK1 by AMPK regulates translocation of ULK1 to mitochondria and mitophagy. FEBS Lett. 2015;589(15):1847-54. doi: 10.1016/j.febslet.2015.05.020. PubMed PMID: 25980607.

45. Kinoshita E, Kinoshita-Kikuta E, Takiyama K, Koike T. Phosphate-binding tag, a new tool to visualize phosphorylated proteins. Mol Cell Proteomics. 2006;5(4):749-57. doi: 10.1074/mcp.T500024-MCP200. PubMed PMID: 16340016.

46. Sarraf SA, Raman M, Guarani-Pereira V, Sowa ME, Huttlin EL, Gygi SP, et al. Landscape of the PARKIN-dependent ubiquitylome in response to mitochondrial depolarization. Nature. 2013;496(7445):372-6. doi: 10.1038/nature12043. PubMed PMID: 23503661; PubMed Central PMCID: PMCPMC3641819.

47. Gegg ME, Cooper JM, Chau KY, Rojo M, Schapira AH, Taanman JW. Mitofusin 1 and mitofusin 2 are ubiquitinated in a PINK1/parkin-dependent manner upon induction of mitophagy. Hum Mol Genet. 2010;19(24):4861-70. doi: 10.1093/hmg/ddq419. PubMed PMID: 20871098; PubMed Central PMCID: PMCPMC3583518.

48. Chan NC, Salazar AM, Pham AH, Sweredoski MJ, Kolawa NJ, Graham RL, et al. Broad activation of the ubiquitin-proteasome system by Parkin is critical for mitophagy. Hum Mol Genet. 2011;20(9):1726-37. doi: 10.1093/hmg/ddr048. PubMed PMID: 21296869; PubMed Central PMCID: PMCPMC3071670.

49. Lazarou M, Narendra DP, Jin SM, Tekle E, Banerjee S, Youle RJ. PINK1 drives Parkin self-association and HECT-like E3 activity upstream of mitochondrial binding. J Cell Biol. 2013;200(2):163-72. doi: 10.1083/jcb.201210111. PubMed PMID: 23319602; PubMed Central PMCID: PMCPMC3549971.

50. Joo JH, Dorsey FC, Joshi A, Hennessy-Walters KM, Rose KL, McCastlain K, et al. Hsp90-Cdc37 chaperone complex regulates Ulk1- and Atg13-mediated mitophagy. Mol Cell. 2011;43(4):572-85. doi: 10.1016/j.molcel.2011.06.018. PubMed PMID: 21855797; PubMed Central PMCID: PMCPMC3485687.

51. Alers S, Loffler AS, Paasch F, Dieterle AM, Keppeler H, Lauber K, et al. Atg13 and FIP200 act independently of Ulk1 and Ulk2 in autophagy induction. Autophagy. 2011;7(12):1423-33. PubMed PMID: 22024743.

52. Xiao B, Sanders MJ, Carmena D, Bright NJ, Haire LF, Underwood E, et al. Structural basis of AMPK regulation by small molecule activators. Nat Commun. 2013;4:3017. doi: 10.1038/ncomms4017. PubMed PMID: 24352254; PubMed Central PMCID: PMCPMC3905731.

53. Bylund L, Kytola S, Lui WO, Larsson C, Weber G. Analysis of the cytogenetic stability of the human embryonal kidney cell line 293 by cytogenetic and STR profiling approaches. Cytogenet Genome Res. 2004;106(1):28-32. doi: 10.1159/000078556. PubMed PMID: 15218237.

54. Yan J, Kuroyanagi H, Tomemori T, Okazaki N, Asato K, Matsuda Y, et al. Mouse ULK2, a novel member of the UNC-51-like protein kinases: unique features of functional domains. Oncogene. 1999;18(43):5850-9. doi: 10.1038/sj.onc.1202988. PubMed PMID: 10557072.

55. Alers S, Loffler AS, Wesselborg S, Stork B. The incredible ULKs. Cell Commun Signal. 2012;10(1):7. doi: 10.1186/1478-811X-10-7. PubMed PMID: 22413737; PubMed Central PMCID: PMCPMC3330011.

56. Heo JM, Ordureau A, Paulo JA, Rinehart J, Harper JW. The PINK1-PARKIN Mitochondrial Ubiquitylation Pathway Drives a Program of OPTN/NDP52 Recruitment and TBK1 Activation to Promote Mitophagy. Mol Cell. 2015;60(1):7-20. doi: 10.1016/j.molcel.2015.08.016. PubMed PMID: 26365381; PubMed Central PMCID: PMCPMC4592482.

57. Lazarou M, Sliter DA, Kane LA, Sarraf SA, Wang C, Burman JL, et al. The ubiquitin kinase PINK1 recruits autophagy receptors to induce mitophagy. Nature. 2015;524(7565):309-14. doi: 10.1038/nature14893. PubMed PMID: 26266977; PubMed Central PMCID: PMCPMC5018156.

58. Richter B, Sliter DA, Herhaus L, Stolz A, Wang C, Beli P, et al. Phosphorylation of OPTN by TBK1 enhances its binding to Ub chains and promotes selective autophagy of damaged mitochondria. Proc Natl Acad Sci U S A. 2016;113(15):4039-44. doi: 10.1073/pnas.1523926113. PubMed PMID: 27035970; PubMed Central PMCID: PMCPMC4839414.

59. Helgason E, Phung QT, Dueber EC. Recent insights into the complexity of Tank-binding kinase 1 signaling networks: the emerging role of cellular localization in the activation and substrate specificity of TBK1. FEBS Lett. 2013;587(8):1230-7. doi: 10.1016/j.febslet.2013.01.059. PubMed PMID: 23395801.

60. Toyama EQ, Herzig S, Courchet J, Lewis TL, Jr., Loson OC, Hellberg K, et al. Metabolism. AMP-activated protein kinase mediates mitochondrial

fission in response to energy stress. Science. 2016;351(6270):275-81. doi: 10.1126/science.aab4138. PubMed PMID: 26816379; PubMed Central PMCID: PMCPMC4852862.

61. Witters LA. The blooming of the French lilac. J Clin Invest. 2001;108(8):1105-7. doi: 10.1172/JCI14178. PubMed PMID: 11602616; PubMed Central PMCID: PMCPMC209536.

62. Zhou G, Myers R, Li Y, Chen Y, Shen X, Fenyk-Melody J, et al. Role of AMP-activated protein kinase in mechanism of metformin action. J Clin Invest. 2001;108(8):1167-74. doi: 10.1172/JCI13505. PubMed PMID: 11602624; PubMed Central PMCID: PMCPMC209533.

63. Shaw RJ, Lamia KA, Vasquez D, Koo SH, Bardeesy N, Depinho RA, et al. The kinase LKB1 mediates glucose homeostasis in liver and therapeutic effects of metformin. Science. 2005;310(5754):1642-6. doi: 10.1126/science.1120781. PubMed PMID: 16308421; PubMed Central PMCID: PMCPMC3074427.

64. Wang CP, Lorenzo C, Habib SL, Jo B, Espinoza SE. Differential effects of metformin on age related comorbidities in older men with type 2 diabetes. J Diabetes Complications. 2017;31(4):679-86. doi: 10.1016/j.jdiacomp.2017.01.013. PubMed PMID: 28190681.

65. Markowicz-Piasecka M, Sikora J, Szydlowska A, Skupien A, Mikiciuk-Olasik E, Huttunen KM. Metformin - a Future Therapy for Neurodegenerative Diseases. Pharm Res. 2017. doi: 10.1007/s11095-017-2199-y. PubMed PMID: 28589443.

66. Lu M, Su C, Qiao C, Bian Y, Ding J, Hu G. Metformin Prevents Dopaminergic Neuron Death in MPTP/P-Induced Mouse Model of Parkinson's Disease via Autophagy and Mitochondrial ROS Clearance. Int J Neuropsychopharmacol. 2016;19(9). doi: 10.1093/ijnp/pyw047. PubMed PMID: 27207919; PubMed Central PMCID: PMCPMC5043649.

67. Kuan YC, Huang KW, Lin CL, Hu CJ, Kao CH. Effects of metformin exposure on neurodegenerative diseases in elderly patients with type 2 diabetes mellitus. Prog Neuropsychopharmacol Biol Psychiatry. 2017;79(Pt B):77-83. doi: 10.1016/j.pnpbp.2017.06.002. PubMed PMID: 28583443.

68. Moreira PI. Metformin in the diabetic brain: friend or foe? Ann Transl Med. 2014;2(6):54. doi: 10.3978/j.issn.2305-5839.2014.06.10. PubMed PMID: 25333029; PubMed Central PMCID: PMCPMC4200667.

69. Fujiwara M, Marusawa H, Wang HQ, Iwai A, Ikeuchi K, Imai Y, et al. Parkin as a tumor suppressor gene for hepatocellular carcinoma. Oncogene. 2008;27(46):6002-11. doi: 10.1038/onc.2008.199. PubMed PMID: 18574468.

70. Bernardini JP, Lazarou M, Dewson G. Parkin and mitophagy in cancer. Oncogene. 2017;36(10):1315-27. doi: 10.1038/onc.2016.302. PubMed PMID: 27593930.

71. Ran FA, Hsu PD, Wright J, Agarwala V, Scott DA, Zhang F. Genome engineering using the CRISPR-Cas9 system. Nat Protoc. 2013;8(11):2281-308. doi: 10.1038/nprot.2013.143. PubMed PMID: 24157548; PubMed Central PMCID: PMCPMC3969860.